Inorganic Chemistry

Article

pubs.acs.org/IC

Ru(II) and Os(II) Complexes Based on Terpyridyl-Imidazole Ligand Rigidly Linked to Pyrene: Synthesis, Structure, Photophysics, Electrochemistry, and Anion-Sensing Studies

Dinesh Maity, Chanchal Bhaumik, Debiprasad Mondal, and Sujoy Baitalik*

Department of Chemistry, Inorganic Chemistry Section, Jadavpur University, Kolkata 700032, India

Supporting Information

ABSTRACT: We report in this work a new family of bis-tridentate ruthenium(II) and osmium(II) complexes bearing a terpyridyl ligand rigidly link to pyrenyl-benzimidazole moiety (tpy-HImzPy = 10-(4-[2,2':6',2"-terpyridine]terpyridin-4'-yl-phenyl)-9*H*-9,11-diaza-cyclopenta[*e*]pyrene) along with other tridentate ligands such as 4′-(2-naphthyl)-2,2′:6′,2″-terpyridine (tpy-NaPh) and 2,6-bis(benzimidazole-2-yl)pyridine (H_2pbbzim). All the complexes are thoroughly characterized by their elemental analysis, ESI mass spectrometry, and ^{1}H NMR spectroscopy. The molecular structures of two complexes [Ru(tpy-HImzPy)$_2$](ClO$_4$)$_2$ (**3**) and [(pbbzim)Ru-(tpy-HImzPy)] (**2a**) in the solid state were determined by X-ray crystallography. The absorption, steady-state, and time-resolved luminescence and electrochemical properties of all the four compounds have been studied. On excitation at their MLCT bands, all four compounds exhibit moderately strong room-temperature luminescence with lifetimes ranging between 3.8 and 161.1 ns in aerated condition, whereas in the deaerated (N_2 purged) condition, the lifetimes vary between 8.2 and 199.1 ns, depending upon the nature of the solvents. The presence of imidazole N−H protons in all the complexes motivates us to study anion sensing properties of the complexes in solution through different channels. Spectrophotometeric, fluorometric, ^{1}H NMR spectroscopic, and cyclic voltammetric studies of the complexes in presence of anions reveal that the complexes sense principally F$^-$, CN$^-$, and to a lesser extent for AcO$^-$. Multichannel anion sensing studies also indicate that anion-induced deprotonation of the imidazole N−H protons occur in all four compounds. The equilibrium constant of this deprotonation steps have been estimated from UV−vis absorption and emission titration data. Anion-induced modulation of lifetimes makes all the four complexes suitable for lifetime-based sensors for selective anions.

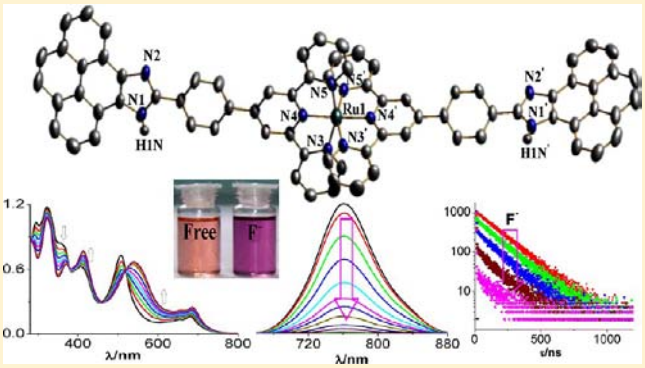

INTRODUCTION

Ruthenium(II) and osmium(II) polypyridyl complexes show outstanding photophysical and electrochemical properties which make them suitable for the use in various light-induced applications.[1−3] Among the polypyridine ligands, 2,2′-bipyridine (bpy), 1,10-phenanthroline (phen), or 2,2′:6′,2″-terpyridine (tpy) are widely used to coordinate ruthenium(II) and osmium(II).[1−3] Significant modulation of the physicochemical properties of these complexes can be done by changing the structural and electronic nature of these ligands.[2] It has been observed from the literature that ligands derived from bpy and phen moieties are superior over tpy as far as the photophysical properties of ruthenium(II) complexes are concerned.[1−3] In fact [Ru(bpy)$_3$]$^{2+}$ and [Ru(phen)$_3$]$^{2+}$ show intense and long-lived luminescence at room temperature, whereas [Ru(tpy)$_2$]$^{2+}$ is almost nonluminescent.[4] From the structural viewpoint, the bis-tridentate complexes are much better as they are free from isomerism compared with tris-bidentate chelates and functionalization at the central position of the tpy ligand leads to linear rodlike assemblies.[5,6] In this context, several attempts have been done by various research groups to increase the room temperature luminescence as well as excited-state lifetimes of bis-tridentate ruthenium(II) complexes. Because one of the reasons of the short excited-state lifetimes is the small energy gap between the emitting ^{3}MLCT state and nonemitting ^{3}MC states, increasing the energy gap between these two states would be very much beneficial. This can be obtained by using different electron withdrawing[7] and electron donating substituents or using cyclometalating ligand or by using extended π-delocalizing moieties at the ligands.[8] In all cases, strategies were adopted to manipulate primarily the energy of the emitting ^{3}MLCT state.[9−13] In this context, we recently reported an interesting class of bis-tridentate ruthenium(II) and osmium(II) complexes with different terpyridyl-imidazole ligands in combination with other tridentate ligands that displayed moderately strong room temperature luminescence with enhanced lifetimes compared with prototype [Ru-(tpy)$_2$]$^{2+}$.[14]

Received: June 22, 2013
Published: November 22, 2013

The studies of the bichromophoric systems consisting of ruthenium(II) diimine complex and a covalently linked polycyclic hydrocarbon such as pyrene have receiving increasing interest in recent years.[15−24] In this context, several diimine ligands either directly coupled to pyrene or linked by a spacer have been prepared, and the photophysical and photochemical properties of their ruthenium(II) and osmium(II) complexes have been carefully and systematically investigated by several research groups such as Roger, Sasse, Schmehl, Thummel, Castellano, Wilson, Schlüter, and co-workers.[15−24] It has been demonstrated that the lifetimes in these dyads are modulated in part by the spacer but are ultimately controlled by the relative triplet energy levels of the metal diimine and pyrene chromophores.[17−19] The mutual communication between these constituent components in such molecules are not only interesting from a theoretical perspective with regard to intramolecular electron and energy transfer processes but also of potential interest for luminescence-based analytical applications and for molecular device research.[25−27] In contrast to most of the reported pyrene-diimine ligands, where the pyrene chromophore is connected to a diimine complexation units such as bpy or phen, pyrene-triimine ligands where terpyridyl complexation site is rigidly linked to pyrene chromophores are relatively sparse in the literature.[20,24,28] In this context, we synthesize and fully characterize a new ditopic ligand 10-(4-[2,2′:6′,2″-terpyridine]-terpyridin-4′-yl-phenyl)-9*H*-9,11-diaza-cyclopenta[e]pyrene (tpy-HImzPy). It is interesting to note that in the novel ligand a pyrenyl-imidazole moiety has been fused at the 4′-position of the tpy which can be utilized for the synthesis of monometallic ruthenium(II) and osmium(II) complexes. Moreover, all the complexes contain imidazole NH proton(s) in the second coordination sphere. Thus, there remains scope for anion sensing studies of all the complexes through different channels by taking advantage of these acidic NH protons. A lot of studies reported in the literature showed that $[Ru^{II}(bpy)_3]^{2+}$ (bpy = 2,2′-bipyridine) moiety covalently linked to a variety of receptors containing amide or imidazole N−H fragments as hydrogen-bond donors has been extensively investigated as an optical reporter for anion sensing.[29−32] By contrast, studies involving $[Ru(tpy)_2]^{2+}$-type complexes are extremely rare.[14,33,34] As part of our interest in exploring new terpyridine ligands and their ruthenium(II) complexes with improved room temperature photophysical properties and in our endeavor to develop triple channel anion sensors utililizing the less explored $[Ru(tpy)_2]^{2+}$-type chromophores, we have studied in detail structural, spectroscopic, and physicochemical properties of a series of both homo- and hetroleptic bis-tridentate ruthenium(II) and osmium(II) complexes derived from hybrid tpy-pyrenyl-imidazole ligand (tpy-HImzPy) and their interactions with several anions, including F^-, CN^-, and AcO^-. It would be of interest to see that all the complexes will exhibit moderately strong luminescence at room temperature with their lifetimes in the subnanosecond time domain. Moreover, remarkable changes in the photophysical properties as well as the color of the complexes can be seen consequent to receptor−anion interactions.

EXPERIMENTAL SECTION

Materials. All commercially available chemicals were purchased from Sigma Aldrich Chemical Co. and used as received. Pyrene-4,5-dione was prepared from pyrene following a literature procedure.[35] The terpyridine precursors including 4′-(*p*-formylphenyl)-2,2′:6′,2″-terpyridine (tpy-PhCHO) as well as the metal precursors such as $[(tpy{-}NaPh)RuCl_3]$ and $[(H_2pbbzim)RuCl_3]$ were prepared as described previously.[14,36]

Preparation of the Ligand 10-(4-[2,2′:6′,2″-Terpyridine]-terpyridin-4′-yl-phenyl)-9*H*-9,11-diaza-cyclopenta[e]pyrene (tpy-HImzPy). Pyrene-4,5-dione (255 mg, 1.10 mmol), tpy-PhCHO (337 mg, 1.00 mmol), and ammonium acetate (1.6 g, 20 mmol) were suspended in acetic acid (30 mL), and the mixture was refluxed for 2 h with stirring. The reaction mixture was cooled down to room temperature when a pale yellow microcrystalline compound deposited. The precipitated product was collected by filtration and washed thoroughly with water and then air-dried. The compound was purified by recrystallization from 1:1 (v/v) mixture of MeOH and $CHCl_3$, yielding a light yellow crystalline solid. Yield: 385 mg, 70%. Elemental anal. Calcd for tpy-HImzPy, $C_{38}H_{23}N_5$: C, 83.04; H, 4.22; N, 12.74. Found: C, 83.01; H, 4.25; N, 12.70. ^{1}H NMR (500 MHz, DMSO-d_6): δ 13.90 (s, 1H, NH imidazole), 8.84 (br, 2H), 8.81 (s, 2H), 8.77 (d, 2H), 8.67 (d, 2H), 8.57 (d, 2H), 8.23 (d, 2H), 8.19 (t, 4H), 8.13 (t, 2H), 8.03 (t, 2H), 7.52 (t, 2H). ^{13}C NMR (500 MHz, DMSO-d_6): δ 172.53, 156.27, 155.43, 149.83, 149.18, 138.30, 137.98, 132.00, 131.72, 128.04, 127.52, 126.81, 125.07, 124.71, 122.34, 121.49, 119.59, and 118.24. ESI-MS (positive, MeOH) m/z = 550.20 (100%) [tpy-HImzPy+H]$^+$ and m/z = 572.19 (3%) [tpy-HImzPy+Na]$^+$.

Synthesis of $[(tpy{-}NaPh)Ru(tpy{-}HImzPy)](ClO_4)_2{\cdot}2H_2O$ (1). A suspension of $[(tpy{-}NaPh)RuCl_3]$ (80 mg, 0.15 mmol) and tpy-HImzPy (82 mg, 0.15 mmol) in 25 mL of ethylene glycol was heated at 180 °C for 12 h with continuous stirring under a nitrogen atmosphere. After the solution was cooled, a saturated aqueous solution of $NaClO_4{\cdot}H_2O$ was added to induce precipitation. The red solid was then filtered and washed thoroughly with water. Purification of the compound was done by performing silica gel column chromatography where acetonitrile was used as eluent. The compound was finally recrstallized from MeCN-MeOH (1:2, v/v) mixture in a slightly acidic medium (1×10^{-4} M $HClO_4$). Yield: 114 mg, 66%. Elemental anal. Calcd. for $[(tpy{-}NaPh)Ru(tpy{-}HImzPy)](ClO_4)_2{\cdot}2H_2O$, $C_{63}H_{44}N_8Cl_2O_{10}Ru$: C, 60.77; H, 3.24; N, 9.00. Found: C, 60.75; H, 3.27; N, 9.02. ^{1}H NMR (500 MHz, DMSO-d_6): δ 14.00 (s, 1H), 9.62−9.60 (m, 4H), 9.18−9.13 (m, 4H), 9.04 (s, 1H), 8.91 (d, 1H), 8.88 (d, 1H), 8.76−8.71 (m, 4H), 8.57 (d, 1H), 8.32−8.29 (m, 3H), 8.23−8.17 (m, 5H), 8.13−8.07 (m, 5H), 7.72−7.69 (m, 2H), 7.62−7.58 (m, 4H), 7.30 (t, 4H). ESI-MS (positive, CH_3CN) m/z = 505.10 (100%) $[(tpy{-}NaPh)Ru(tpy{-}HImzPy)]^{2+}$.

Synthesis of $[(H_2pbbzim)Ru(tpy{-}HImzPy)](ClO_4)_2{\cdot}2H_2O$ (2). Using $[(H_2pbbzim)RuCl_3]$, the complex **2** was obtained by applying the same method as complex **1.** Yield: 106 mg, 63%. Elemental anal. Calcd. for $[(H_2pbbzim)Ru(tpy{-}HImzPy)](ClO_4)_2{\cdot}2H_2O$, $C_{57}H_{40}N_{10}Cl_2O_{10}Ru$: C, 57.19; H, 3.03; N, 11.70. Found: C, 57.17; H, 3.07; N, 11.68. ^{1}H NMR (500 MHz, DMSO-d_6): δ 15.07 (s, 3H), 9.70 (s, 2H), 9.06 (d, 2H), 8.96 (d, 2H), 8.91 (d, 2H), 8.78 (d, 4H), 8.64 (t, 1H), 8.37 (d, 2H), 8.25 (t, 4H), 7.98 (t, 2H), 7.66 (d, 2H), 7.51 (d, 2H), 7.29−7.24 (m, 4H), 7.05 (t, 2H), 6.10 (d, 2H). ESI-MS (positive, CH_3CN) m/z = 481.09 (100%) $[(H_2pbbzim)Ru(tpy{-}HImzPy)]^{2+}$; 960.03 (10%) $[(Hpbbzim)Ru(tpy{-}HImzPy)]^+$.

Synthesis of $[Ru(tpy{-}HImzPy)_2](ClO_4)_2{\cdot}H_2O$ (3). A suspension of $RuCl_3{\cdot}3H_2O$ (32 mg, 0.12 mmol) and tpy-HImzPy (115 mg, 0.21 mmol) in 25 mL of ethylene glycol were stirred at 180 °C for 12 h under nitrogen protection. On cooling down to room temperature, the red solution was treated with saturated aqueous solution of $NaClO_4{\cdot}H_2O$ for inducing precipitation of the compound as the perchlorate salt. The deep red colored precipitate that formed was isolated by filtration and washed with water. The crude product was purified using column chromatography on silica gel using acetonitrile as eluent. On rotary evaporation of the eluent to a small volume (~5 mL), a red compound was obtained which on recrytallization from MeCN-MeOH (1:5, v/v) mixture in slightly acidic condition (1×10^{-4} M $HClO_4$) afforded red crystalline product. Yield: 88 mg, 60%. Elemental anal. Calcd for $[Ru(tpy{-}HImzPy)_2](ClO_4)_2{\cdot}H_2O$, $C_{76}H_{48}N_{10}Cl_2O_9Ru$: C, 64.41; H, 3.27; N, 9.88. Found: C, 64.43; H, 3.29; N, 9.86. ^{1}H NMR (500 MHz, DMSO-d_6): δ 13.98 (s, 2H), 9.61 (s, 4H), 9.17 (d, 4H), 8.92 (d, 2H), 8.88 (d, 2H), 8.76−8.72 (m, 8H), 8.30 (t, 4H), 8.24−

8.17 (m, 8H), 8.10 (t, 4H), 7.61 (d, 4H), 7.32 (t, 4H). ESI-MS (positive, CH_3CN) m/z = 600.14 (100%) $[Ru(tpy\text{-}HImzPy)_2]^{2+}$.

Synthesis of $[Os(tpy\text{-}HImzPy)_2](ClO_4)_2\cdot 2H_2O$ (4). The complex **4** was achieved in the same method as for **3** by using K_2OsCl_6 as the starting material and maintaining the reaction at 200 °C for 24 h, respectively. Yield: 70 mg, 57%. Elemental anal. Calcd. for $[Os(tpy\text{-}HImzPy)_2](ClO_4)_2\cdot 2H_2O$, $C_{76}H_{50}N_{10}Cl_2O_{10}Os$: C, 59.88; H, 3.04; N, 9.19. Found: C, 59.85; H, 3.06; N, 9.17. ^{1}H NMR (500 MHz, DMSO-d_6): δ 13.98 (s, 2H), 9.64 (s, 4H), 9.16 (d, 4H), 8.91 (d, 2H), 8.89 (d, 2H), 8.75 (d, 4H), 8.69 (d, 4H), 8.31−8.29 (m, 4H), 8.24−8.17 (m, 8H), 7.97 (t, 4H), 7.50 (d, 4H), 7.26 (t, 4H). ESI-MS (positive, CH_3CN) m/z = 644.57 (100%) $[Os(tpy\text{-}HImzPy)_2]^{2+}$.

Physical Measurements. Elemental (C, H, and N) analyses of the compounds were done on a Perkin−Elmer 2400II analyzer. ESI-MS were performed on a Micromass Qtof YA 263 mass spectrometer. NMR spectra of the complexes were recorded on either a Bruker 300 or Bruker 500 spectrometer in DMSO−d_6. UV−vis absorption spectra were recorded using a Shimadzu UV 1800 spectrometer at room temperature. Steady state luminescence spectra were obtained by Perkin−Elmer LS55 luminescence spectrometer. Luminescence quantum yields were determined using literature method taking $[Ru(bpy)_3]^{2+}$ as the standard. Luminescence lifetime measurements were carried out by using time−correlated single photon counting set up from Horiba Jobin-Yvon. The luminescence decay data were collected on a Hamamatsu MCP photomultiplier (R3809) and were analyzed by using IBH DAS6 software. For a typical titration experiment, 2 μL aliquots of a TBA salt of different anions were added to a 2.5 mL solution of the complexes. The binding/equilibrium constants were calculated by using eq 1.[37]

$$A_{obs} = (A_0 + A_\infty K[G]_T)/(1 + K[G]_T) \quad (1)$$

where A_{obs} is the observed absorbance, A_0 is the absorbance of the free receptor, A_∞ is the maximum absorbance induced by the presence of a given anionic guest, $[G]_T$ is the total concentration of the guest, and K is the binding constant of the host−guest entity.

Electrochemical measurements were carried out in deaerated acetonitrile with a BAS epsilon electrochemistry system and a three-electrode set up consisting of a platinum or glassy carbon working electrode, a platinum counter electrode, and Ag/AgCl reference electrode. In all the experiments, tetraethylammonium perchlorate (TEAP) was used as background electrolyte. The potentials reported in this study were referenced against the Ag/AgCl electrode, which under the given experimental conditions gave a value of 0.36 V for the Fc/Fc^+ couple.

Crystal Structure Determination of 2a and 3. Single crystals of **2a** for X-ray diffraction were grown from a 1:2 (v/v) mixture of acetone and dichloromethane solution of **2** in the presence of excess TBAF and layering with hexane over the solution. Single crystals of **3**, on the other hand, were grown by diffusing toluene over its acetonitrile-dichloroimethane (9:1, v/v) solution at room temperature. The single crystals of both **2a** and **3** were mounted on the tips of commercially available glass fibers coated with *Fomblin* oil. X-ray single-crystal data collection of the crystals was done at room temperature using a Bruker Smart APEX II CCD diffractometer, equipped with a normal focus, sealed tube X-ray source with graphite monochromated Mo−Kα radiation (λ = 0.71073 Å). The data were integrated using the SAINT[38] program, and the absorption corrections were made with SADABS.[38] All the structures were solved by SHELX-97.[39] Full matrix least-squares refinements were performed on F^2 using SHELX-97 with anisotropic displacement parameters for all non-hydrogen atoms.[39,40] All the hydrogen atoms except the hydrogen of disordered lattice water were fixed geometrically by HFIX command and placed in ideal positions in both cases. Calculations were also carried out using PLATON v1.15,[41] ORTEP-3v2,[42] and WinGX system.[43] Data collection and structure refinement parameters along with crystallographic data for both **2a** and **3** are given in Table 1.

Table 1. Crystallographic Data for 2a and 3[a]

	2a	3
formula	$C_{58}H_{36}Cl_2N_{10}O_2Ru$	$C_{83}H_{54}Cl_2N_{10}O_9Ru$
mol wt	1076.94	1507.33
T (K)	293(2)	293(2)
cryst syst	triclinic	triclinic
space group	$P\bar{1}$	$P\bar{1}$
a (Å)	9.417(5)	11.434(5)
b (Å)	13.291(5)	16.080(5)
c (Å)	23.144(5)	20.049(5)
α (deg)	106.289(5)	109.025(5)
β (deg)	96.429(5)	98.018(5)
γ (deg)	97.578(5)	97.341(5)
V (Å^3)	2722.2(19)	3391(2)
D_c (g cm^{-3})	1.314	1.476
Z	2	2
μ (mm^{-1})	0.437	0.382
$F(000)$	1096	1544
θ range (deg)	2.21- 25.00	2.19- 25.00
data/restraints/params	9578/0/658	11927/1/942
GOF on F^2	0.993	1.138
R1 $[I > 2\sigma(I)]$[b]	0.0624	0.0744
wR2 (all data)[c]	0.2223	0.2223
$\Delta\rho_{max}/\Delta\rho_{min}$ (e Å)	1.043/ −1.034	1.393/-1.110

[a]CCDC reference numbers: 946246 for **2a** and 946245 for **3**. [b]$R1(F) = [\sum ||F_0| - |F_C||/\sum |F_0|]$. [c]$wR2\ (F^2) = [\sum w(F_0^2 - F_C^2)^2/\sum w(F_0^2)^2]^{1/2}$.

RESULTS AND DISCUSSION

Synthesis and Characterization. A new tridentate ligand containing a pyrenyl-imidazole moiety (tpy-HImzPy) was prepared from pyene-4,5-dione and tpy-PhCHO in equimolar quantity under refluxing acetic acid in excess ammonium acetate. Treatment of tpy-HImzPy with stoichiometric amount of appropriate metal precursor in ethylene glycol under refluxing condition leads to the synthesis of the desired homo and heteroleptic metal complexes (Chart 1). The complexes were precipitated as their perchlorate salts by addition of aqueous $NaClO_4.H_2O$ and purifications of the crude products were performed by column chromatography using acetonitrile as the eluent. The main product fraction was collected and recrystallized from MeCN-MeOH mixture under mildly acidic conditions. Characterization of the complexes was done by performing their ESI mass and ^{1}H NMR spectra, and by analyzing the percentage of few selective elements such as C, H, and N. The results of the analytical and spectroscopic measurements are already given in the Experimental Section. Figures S1−S5 (Supporting Information) show the experimental as well as simulated ESI mass spectra of tpy-HImzPy and its metal complexes **1**−**4**. It is nice to see that the experimentally observed peaks in ESI mass spectra of all the compounds fit very well to that of the corresponding calculated patterns.

Description of the Crystal Structures of 2a and 3. Both **2a** and **3** crystallized in the triclinic unit cell of the space group, $P\bar{1}$. Figure 1 shows the ORTEP[42] representation of the complexes and selected bond lengths and bond angles are listed in Table S1 (Supporting Information). The X-ray crystal structures reveal that each Ru(II) center occupies a distorted octahedral geometry, with two tridentate ligands arranged according to a meridional fashion. The distortion from regular octahedron geometry of the complexes is reflected from the

dx.doi.org/10.1021/ic401582m | Inorg. Chem. 2013, 52, 13941−13955

Chart 1

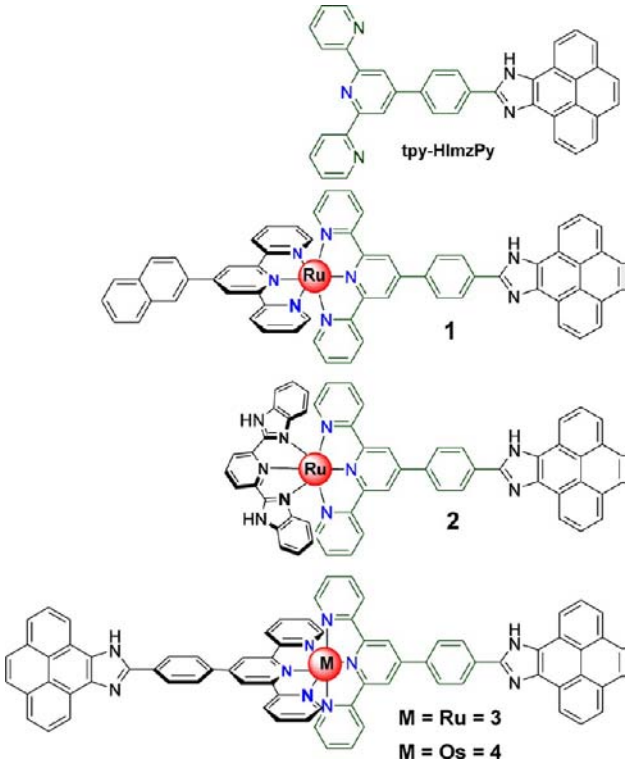

values of different bite angles. The bite angles vary between 77.73(16) and 79.43(14)° for **2a** and between 78.69(17) and 79.31(17)° for **3**. Table S1 in the Supporting Information shows that the interligand trans angle made by N4−Ru1−N8 is 175.03(13)° for **2a** and by N4−Ru1−N4′ for **3** is 178.29(17)°, are very close to linearity, whereas the intraligand trans angles [N3−Ru1−N5, 158.16(15)°, and N6−Ru1−N9, 155.97(16), for **2a** and N3−Ru1−N5, 157.60(17)°, and N3′−Ru1−N5′, 157.84(16)° for **3**] distorts heavily from expected linear values. For **3**, the Ru−N bond distances lie between 1.967(4) and 2.068(4) Å, whereas two types of Ru−N bond lengths are observed in **2a**: the distances associated with H_2pbbzim ligand are within 2.024(4)−2.083(4) Å and are slightly longer compared with the distances associated with tpy-HImzPy moiety (1.955(4)−2.076(4) Å). The observed Ru−N bond distances in both complexes are very close to that of the previously reported Ru(II)-terpyridine type complexes.[8,12,14] It is evident that two outer Ru−N bonds are relatively longer compared with the central Ru−N bonds to each ligand as expected. The dihedral angles between the central and terminal pyridine ring of each terpyridine moiety lie between 0.74° and 9.07° for **3** and between 4.15° and 4.59° for **2a**. The phenyl ring of tpy-HImzPy is twisted with respect to central pyridine by 13.57−26.25° for **3** and 27.33° for **2a**. Again the twist between almost coplanar pyrenyl-imidazole moiety and the plane of the phenyl group are 6.19 and 23.55° for **3** and 8.03° and for **2a**.

Crystal structure analysis of **2a** and **3** indicates two important structural features such as the occurrence of intermolecular aromatic $\pi-\pi$ and CH−π interactions in both the complexes. The ball and stick representation of **3**, presented in Figure S6 (Supporting Information) shows that the phenyl ring adjacent to the imidazole group described by C1−C2−C16−C15−C13−C14 atoms in the pyrenyl moiety is in face−to−face alignment with the identical phenyl ring as well as other phenyl group described by C9−C10−C11−C12−C13−C15 of another pyrenyl unit. The centroid−centroid distances are 4.118 and 3.513 Å, respectively. The phenyl ring (C1−C2−C16−C15−C13−C14) in pyrenyl unit is also involved in face−to−face

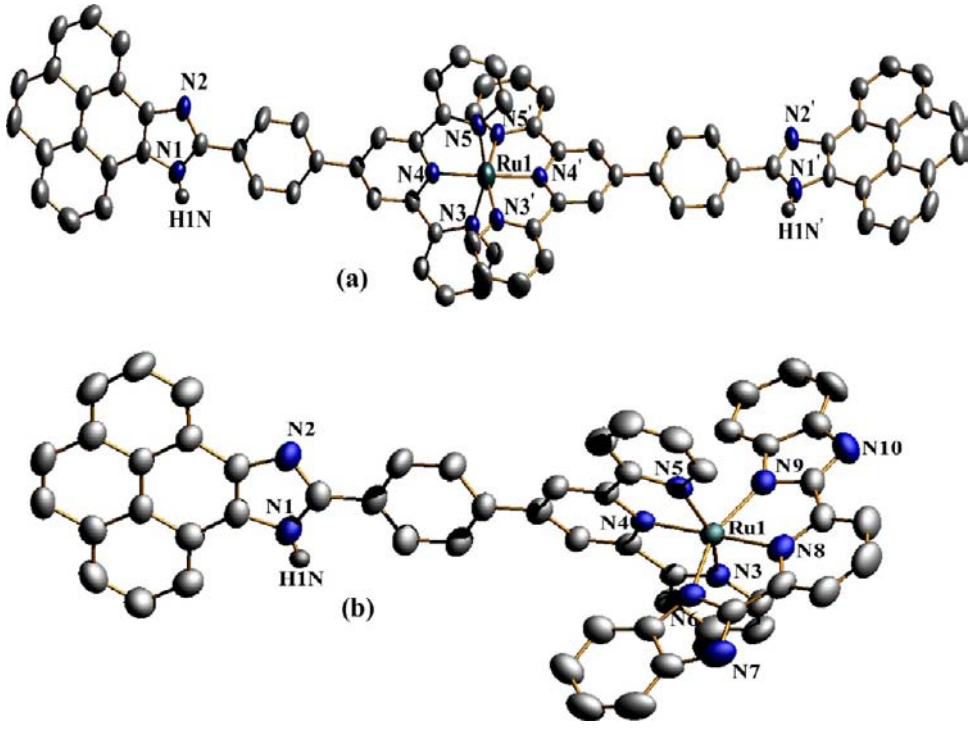

Figure 1. ORTEP[42] representations of (a) **3** and (b) **2a** showing 40% probability of thermal ellipsoid. Hydrogen atoms except imidazole NH and the ClO_4^- counteranions are omitted for clarity.

dx.doi.org/10.1021/ic401582m | *Inorg. Chem.* 2013, 52, 13941−13955

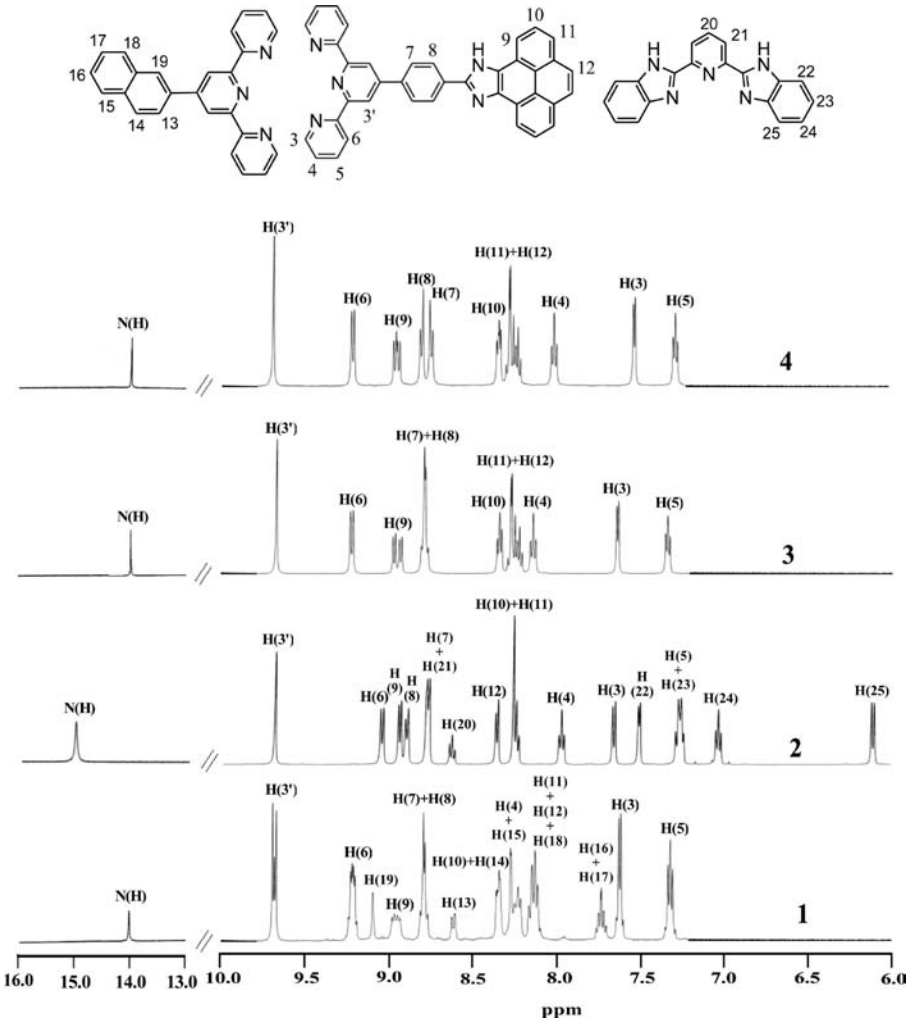

Figure 2. ^{1}H NMR (500 MHz) spectra of 1−4 in DMSO-d_6 at room temperature.

aromatic $\pi-\pi$ interaction with the pyridine ring (N5) of the terpyridine moiety. The centroid−centroid distance between these two rings is 4.154 Å. It is also to be noted that another pyridine ring (N5′) of terpyridine moiety is again in face-to-face alignment with the phenyl ring described by C1′-C2′−C16′−C15′−C13′−C14′ of pyrene with the distance between the two centroid is 4.193 Å. In case of **2a**, the central pyridine ring of pbbzim moiety coordinated to Ru^{II} by N8 is in $\pi-\pi$ interaction with the pyridine ring of another identical N8 unit with the centroid−centroid distance between these two pyridine rings is 4.092 Å (see Figure S7 in the Supporting Information). Similar $\pi-\pi$ interaction also occurs among the phenyl group of pbbzim moiety described by C39−C44 carbon atoms and the centroid−centroid distance is 4.246 Å (see Figure S7 in the Supporting Information). The central pyridine ring of tpy-HImzPy is in face-to-face alignment with the phenyl rings (C6−C7−C8−C9−C15−C16) of pyrenyl moiety of another tpy-HImzPy unit and the distance is 4.456 Å. Again the phenyl ring (C18−C23) of tpy-HImzPy is in face−to−face alignment simultaneously with the two phenyl ring (C1−C2−C16−C15−C13−C14 and C2−C3−C4−C5−C6−-C16) of another pyrenyl unit. The centroid-centroid distances are 3.672 and 4.243 Å. There are also other weak aromatic $\pi-\pi$ interactions as shown in Figure S7 and Table S2 (Supporting Information).

Figures S8 and S9 (Supporting Information), on the other hand, show the occurrence of CH−π interactions in both **2a** and **3**. In **3**, two hydrogen (H23 and H23′) atoms of the central phenyl ring (C18−C23 and C18′−C23′) of tpy-HImzPy unit is in close proximity to the pyridyl ring with the N3′ and N3 atoms of another unit. The distances between H23 and H23′ and the centroid of the pyridyl ring are indeed short and measured to be 2.88 Å and 2.92 Å, respectively (see Table S3 in the Supporting Information). Moreover, H32 atom of a pyridyl ring with N3 nitrogen atom is in close proximity (2.65 Å) to the phenyl ring (C9′−C10′−C11′−C12′−C13′−C15′) of the pyrenyl moiety. In **2a**, the hydrogen atom (H40) of the phenyl ring of benzimidazole moiety described by C39−C44 carbon atoms interacts intramolecularly with the π clouds of the central pyridyl rings, whereas H43 is involved in intermolecular CH−π interactions with pyridyl ring with N5 nitrogen. The corresponding distances between hydrogen atoms to centroid of pyridine rings are 2.87 and 2.88 Å (see Table S3 in the Supporting Information).

NMR Spectroscopy. The ligand tpy-HImzPy and all the complexes (**1**−**4**) were unambiguously characterized by NMR spectroscopy. Figure 2 shows the ^{1}H NMR spectra of complexes **1**−**4** in DMSO-d_6. The COSY spectra (see Figures S10−S12 in the Supporting Information) were much useful to locate spin couplings in the aromatic protons of tpy-HImzPy,

dx.doi.org/10.1021/ic401582m | Inorg. Chem. 2013, 52, 13941−13955

tpy-NaPh, and H_2pbbzim moieties bound to the metal center. The tentative assignments of different protons in the ligand as well as in the metal complexes are summarized in Table S4 (Supporting Information). Because of the presence of same ligands in the homoleptic **3** and **4** complexes, a single set of resonances are observed for each proton in their ^{1}H NMR spectra. By contrast, the spectra of **1** and **2** are somewhat more complex because of different protons arising from dissimilar ligands. Figure 2 shows that all the complexes display a singlet lying between 13.98 and 15.07 ppm which is assigned to imidazole NH proton(s) of tpy-HImzPy and H_2pbbzim ligands. The chemical shift values indicate the formation of strong hydrogen bonding between the coordinated NH proton(s) with DMSO-d_6. The most upfield resonance occurs as a doublet at 6.10 ppm for **2**. This doublet is due to H25 of H_2pbbzim as this proton is heavily shielded by the ring current of the adjacent pyridine ring. The chemical shifts of the pyrene ring protons attached to the imidazole moiety are characterized by the signals in the region 8.07−8.96 ppm, assigned on the basis of coupling constants and chemical shifts. As can be seen that the chemical shifts of H3′, H6, H7, and H8 protons shifted to downfield region while the pyrene ring protons and H4 of terpyridine moiety are almost unaffected by coordination. H3 proton of tpy moiety in tpy-HImzPy shifts to significantly upfield region as this proton lies above the shielding zone. Single-crystal X-ray structures (**2a** and **3**) described above indicates that the pyrene moiety has indeed been effective at aggregating the discrete Ru(II) terpyridyl complexes into polymeric chain in the solid-state. In order to check whether aggregation occurs in the solution state, serial NMR dilution experiments were performed on the complexes in DMSO-d_6 solutions, starting from a saturated solution in DMSO-d_6. Practically, the spectral patterns and the chemical shift values of different protons remain unaltered, implying that the aromatic hydrocarbon moiety do not cause aggregation in solution.

Electronic Absorption Spectroscopic Studies. The UV−vis absorption spectrum of free ligand **tpy-HImzPy** in DMSO is shown in Figure 3, whereas that of **1**−**4** in CH_3CN

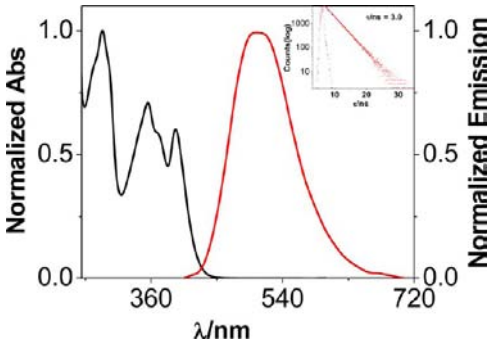

Figure 3. Overlay of absorption and emission spectra of **tpy-HImzPy** at room temperature in dimethylsulfoxide. The inset shows the luminescence decay profile of **tpy-HImzPy**.

are presented in Figure 4. The corresponding λ_{max} values as well as molar extinction coefficients (ε) of all compounds are listed in Table 2. Data for reference mononuclear model complexes are also shown for comparison. The electronic absorption spectrum of **tpy-HImzPy** in DMSO exhibits intense band at 294, 356, and 394 nm that can be ascribed to $\pi\rightarrow\pi^*$ transitions of the tpy and pyrenyl-imidazole unit. The electronic spectra of **1**−**4** exhibit a relatively intense band in UV region and

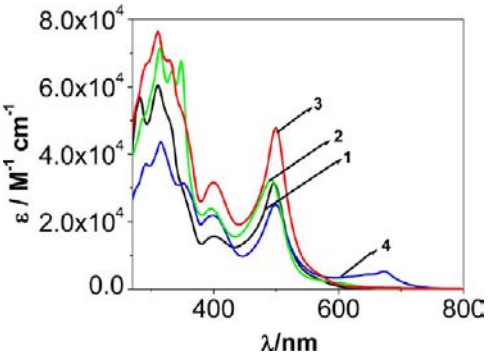

Figure 4. Absorption spectra of **1**−**4** in acetonitrile at room temperature.

moderately intense band in the visible region. The absorption bands of the complexes were assigned by comparing with the UV−vis absoprtion spectra of $[M(tpy)_2]^{2+}$ and related bis-tridentate M(II) (M = Ru^{II} and Os^{II}) type complexes.[2−5,14] The intense high energy band of all the complexes in the UV region between 282 and 400 nm (ε = 15 660−76 080 M^{-1} cm^{-1}) are dominated by $\pi-\pi^*$ and internal transitions of the coordinated ligands and moderately intense band in the visible region lying in the range of 493−500 nm (ε = 25 070−47 660 M^{-1} cm^{-1}) are due to metal-to-ligand [M($d\pi$) to tpy-HImzPy(π^*)] charge transfer (MLCT) transition. It is of interest to note that upon coordination of tpy-HImzPy with metal (Ru^{II} and Os^{II}), the ligand-centered bands are considerably shifted to longer wavelength due to substantial stabilization of its π^* orbital (Figure 4). In **4** additional band is observed around 674 nm, which seems to be due to spin-forbidden MLCT transition from $^1[Os^{II}(d\pi)^6]$ to $^3[Os^{II}(d\pi)^5$tpy-HImzPy$(\pi^*)^1]$. In **2**, a weak and broad shoulder is also observed at ∼600 nm due to $^1[Ru^{II}(d\pi)^6] \rightarrow {}^3[Ru^{II}(d\pi)^5$tpy-HImzPy$(\pi^*)^1]$ transitions.[2−5,14,44] The magnitude of molar extinction coefficient (ε) of the spin forbidden ^{3}MLCT transition is much more in **4** compared to **2** as expected. It is worth noting that the MLCT bands of the complexes in the present study are much more intense compared with bis-terpyridine complexes of Ru(II) and Os(II). Thus the present complexes may be useful building blocks for various light-induced applications. We again performed the dilution experiments of the complexes over 1 × 10^{-3} to 1 × 10^{-5} M concentration range in CH_3CN. Practically no change in their peak maxima, shape or extinction coefficients occur, which again is consistent with no solution aggregation as was also seen with the NMR.

Emission Spectroscopic Studies. All the complexes exhibit a fairly strong emission in acetonitrile fluid solution as well as in solid powder state at room temperature and in EtOH−MeOH (4:1, v/v) rigid matrix at 77 K. Figure 5 represents the luminescence spectra of the complexes (**1**−**4**) in different phases. The luminescence data for all complexes along with those related compounds for comparison are listed in Table 2. The emission spectrum of **tpy-HImzPy**, already presented in Figure 3, shows that on excitation at 390 nm, it fluoresce strongly (Φ = 0.24) at 508 nm in DMSO with lifetime of 3.0 ns. When excited at their MLCT band (∼500 nm), all the complexes exhibit strong luminescence with their band position lying between 658 nm (**1**) and 750 nm (**4**) in solution at 298 K, between 635 nm (**1**) and 763 nm (**4**) in solid state at 298 K, and between 643 nm (**1**) and 734 nm (**4**) at 77 K. Comparing with the literature data of the related compounds, it

dx.doi.org/10.1021/ic401582m | Inorg. Chem. 2013, 52, 13941−13955

Table 2. Spectroscopic and Photophysical Data for Complexes 1−4 in Acetonitrile Solutions

		luminescence						
		at 298 K[a]					at 77 K[b]	
compds	absorption λ_{max} (nm) (ε ($M^{-1}cm^{-1}$))	λ_{max} (nm)	τ (ns)	Φ ($\times 10^{-3}$)	k_r ($\times 10^5$ s^{-1})	k_{nr} ($\times 10^7$ s^{-1})	λ_{max} (nm)	Φ
1	497(31310), 401(15660) 332 (sh)(49150), 311(60460) 282(56770)	658	1.5, 3.8	4.9	32.5, 12.8	66.3, 26.2	643	0.21
2	493(32300), 396(23750) 349(67050), 334(64300) 314(71200), 286(sh)(50420)	682	7.9, 19.8	21.7	27.5, 11.0	12.4, 4.9	682	0.25
3	500(47660), 400(31580) 328(sh)(67890), 310(76080) 294(sh)(67080)	659	2.1, 4.8	6.6	31.3, 13.7	47.3, 20.7	646	0.18
4	674(br)(5200), 499(25070) 400(21800), 349(sh)(31200) 316(43400), 294(36670)	750	112.5	212.4	18.9	0.7	734	0.33
tpy-HImzPy[c]	394(32980), 372(sh)(31420), 356(38890), 294(54890)	508	3.0	240.0				
$[Ru(tpy)_2]^{2+}$[d]	474(10400)	629	0.25	≤0.05	0.04	90.9	598	
$[Ru(tpy\text{-}PhCH_3)_2]^{2+}$[d]	490(28000)	640	<5.0	≤0.03			628, 681(sh)	
$[Ru(H_2pbbzim)_2]^{2+}$[e]	475(17400)							
$[Os(tpy)_2]^{2+}$[d]	657(3650) 477(13750)	718	269	14.0			689	0.124
$[Os(tpy\text{-}PhCH_3)_2]^{2+}$[d]	667(6600) 490(26000)	734	220	21.0			740	0.049

[a]In CH_3CN. [b]MeOH-EtOH(1:4) glass. [c]In DMSO. [d]Data from ref 2. [e]Data from ref 45.

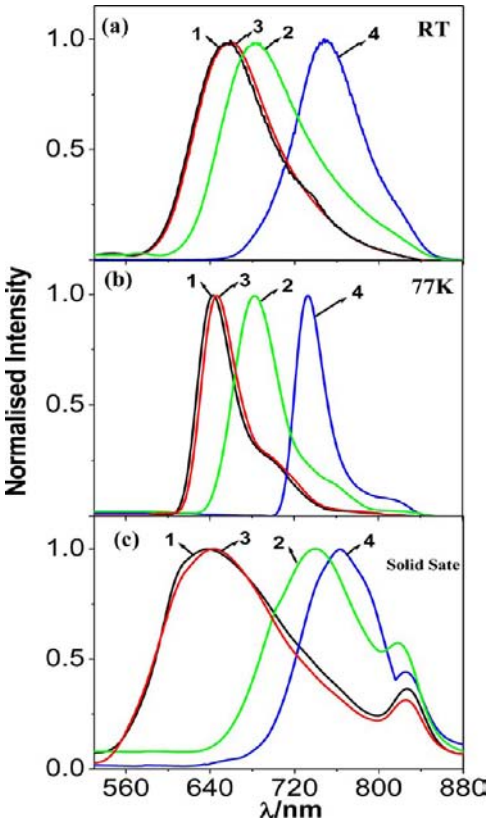

Figure 5. Photoluminescence spectra of **1−4** at room temperature in acetonitrile (a), at 77 K in methanol−ethanol (1:4) glass (b), and in solid powder state (c).

is evident that luminescence originates from the lowest laying ^{3}MLCT excited state of the complexes. Thus, one important observation is that the strong luminescence band at 508 nm due to free **tpy-HImzPy** is completely quenched in the metal complexes by the energy transfer to the corresponding metal−based units, which exhibit their characteristic MLCT phosphorescence. Time-resolved luminescence spectra of the complexes have also been acquired at room temperature and their decay profiles are shown in Figure 6 and Figure S13 (Supporting Information). All the three Ru(II) complexes exhibit biexponential radiative decay, with an initial room-temperature luminescence lifetimes in the range of 1.5−7.9 ns in acetonitrile and between 0.8 and 2.3 ns in dimethysulfoxide followed by a relatively longer lived component with excited state lifetime ranging between 3.8 and 19.8 ns in acetonitrile and between 7.4 and 45.7 ns in dimethylsulfoxide (Figure 6 and Figure S13, Supporting Information). The first component may be attributed to the ^{3}MLCT state based on the **tpy-HImzPy** unit, and the second component probably arises from the equilibrium with the triplet state of the fused pyrene moiety which repopulates the ^{3}MLCT state after the initial emission.[8,46] Thus, one of the important aspects of this study is the observation of moderately strong room temperature luminescence with reasonably long excited state lifetimes of the ruthenium(II) complexes **1−3** in solution compared with practically nonluminescent $[Ru(tpy)_2]^{2+}$ (0.25 ns) [2] or $[Ru(H_2pbbzim)_2]^{2+}$. Lifetime of the Os(II) complex (**4**), on the other hand, is relatively long: 112.5 ns in acetonitrile and 161.1 ns in dimethysulfoxide, as expected. It is also interesting to note that introduction of pyrenyl-imidazole moiety at the 4′-position of terpyridine does not lower the excited-state energy of the complexes significantly.

To address the issue whether the dissolved oxygen can play any role on their excited state behaviors, we measured the lifetimes of complexes **1−4** in both aerated and deaerated (nitrogen-purged) acetonitrile and dimethysulfoxide. For aerated solutions the excited state decays of the complexes are relatively faster compared with the deaerated solutions in

dx.doi.org/10.1021/ic401582m | Inorg. Chem. 2013, 52, 13941−13955

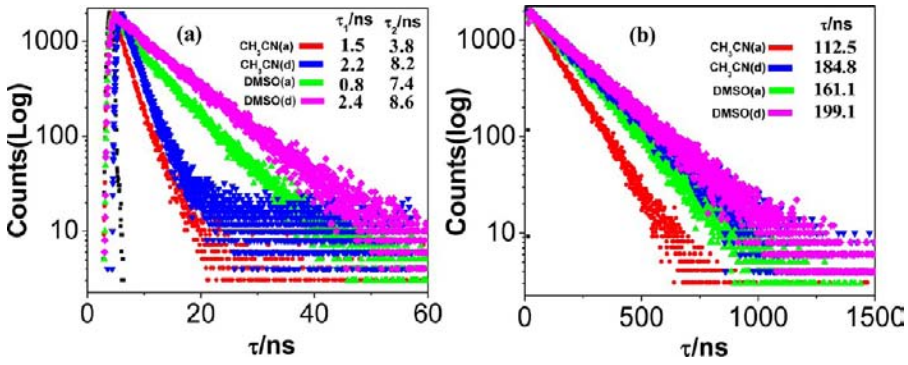

Figure 6. Time-resolved photoluminescence decays of (a) **1** and (b) **4** at room temperature in acetonitrile and dimethylsulfoxide in both aerated and deaerated (nitrogen purged) obtained with 440 nm excitation. Lifetimes of the complexes are shown in the insets of the figure.

both solvents. The excited state lifetimes vary between 3.8 and 161.1 ns in aerated condition, whereas in the deaerated condition, the lifetimes range between 8.2 and 199.1 ns, depending upon the nature of the solvents (Figure 6 and Figure S13, Supporting Information). These data clearly demonstrate that lifetimes of the complexes are quenched significantly by dissolved oxygen particularly in acetonitrile.

The luminescence maxima of the complexes shifted to higher energy region along with remarkable enhancement of luminescence intensities when the solutions of the complexes were frozen at 77 K. The E_{00} of the ^{3}MLCT states of the complexes were approximated from their luminescence maxima at 77 K. The E_{00} values of the complexes lie in the range between 1.69 and 1.93 eV. In the luminescence spectra of the complexes at 77 K, clear signature of vibronic progression are observed in the lower energy region with spacing between them varying in the range of 1225−1488 cm^{-1}, typical of the aromatic stretching vibrations of the coordinated ligands in the complexes.[2−5,14]

It is evident from the literature data that the decay of the excited state of Ru(II) and Os(II) polypyridine complexes takes place by the competition between radiative and radiationless deactivations. The ^{3}MLCT excited states of these complexes are sufficiently weak emitters so that their lifetimes are dominated by nonradiative decay and in this limit the decay can usually be represented by the following relationship.

$$k_{nr} = k_{nr}^{0} + k'_{nr} \quad (2)$$

where k_{nr} represents overall radiationless decay constant, k_{nr}^{0} represents direct decay from the excited ^{3}MLCT state to the ground state, and k'_{nr} represents the crossing from the lowest ^{3}MLCT state to the ^{3}MC. The value of k'_{nr} is very much dependent on the energy difference between ^{3}MLCT and ^{3}MC states. The energy gap between ^{3}MLCT and ^{3}MC states is generally very small for bis-tridentate ruthenium(II) at room temperature because of the unfavorable bite angles of the tridentate ligands around the metal center in an octahedral geometry. As a result of the this small energy gap, Ru(tpy)$_2$-type complexes are notoriously poor emitters at room temperature.[2,3,5,8−10] On the other hand, the energy gap between ^{3}MLCT and ^{3}MC states for bis-tridentate osmium(II) complexes is relatively large as osmium metal induce considerably greater crystal field strength than ruthenium. Thus, thermally activated crossing between ^{3}MLCT and ^{3}MC states get restricted even at room temperature. As a result, complex **4** exhibits longer excited state lifetime (112.5 ns in CH_3CN and 161.1 ns in DMSO) compared to its Ru(II) analogue at room temperature. We believe that the energy of the ^{3}MC states of the complexes in the present study remain constant, while the energy of the emitting ^{3}MLCT state being lowered by rigidly connecting the pyrenyl-imidazole group to the terpyridine moiety. As a result, the efficiency of surface−crossing between ^{3}MLCT and ^{3}MC states is decreased. It may be mentioned that the larger energy gap between ^{3}MLCT and ^{3}MC states may not be the sole factor for long room temperature lifetimes of the complexes.

Electrochemical Properties. The electrochemical characteristics of the complexes (**1**−**4**) along with free **tpy-HImzPy** were investigated by cyclic voltammetry (CV) and square wave voltammetry (SWV) in CH_3CN solutions. CVs and SWVs of the complexes are presented in Figures S14−S15 (Supporting Information) and the pertinent redox data of the complexes as well as reference compounds are summarized in Table 3. All the complexes shows a single one-electron quasi-reversible metal based oxidation (M^{II}/M^{III}) within scan window of 0−1.8 V and a series of quasi-reversible and/or irreversible ligand based reduction within scan window between 0 and −2.2 V. The three Ru(II) complexes show the oxidation potential in the range of 1.05−1.32 V, whereas the Os(II) compound (**4**) is oxidized at relatively smaller potential (0.95 V) as expected. The CVs of the complexes look complicated due to the closeness of the potentials of the Ru^{II} centered oxidation in **1**−**3** and tpy-HImzPy-centered irreversible oxidation (1.4 V). It

Table 3. Electrochemical Data[a] for Complexes 1−4 in Acetonitrile

compds	oxidation[b] $E_{1/2}$(ox) (V)	reduction[c] $E_{1/2}$(red) (V)
1	1.28	−1.13, −1.25, −1.47, −1.78, −1.88
2	1.05	−1.22, −1.47, −1.88, −2.08
3	1.32	−1.22, −1.45, −1.71, −1.87
4	0.95	−1.10, −1.48, −1.75
$[Ru(tpy)_2]^{2+}$[d]	1.30	−1.29, −1.54
$[Ru(tpyPhCH_3)_2]^{2+}$[d]	1.25	−1.24, −1.46
$[Ru(H_2pbbzim)_2]^{2+}$[e]	0.76	−1.40, −1.70
$[Os(tpy)_2]^{2+}$[d]	0.97	−1.25, −1.57
$Os(tpy\text{-}PhCH_3)_2]^{2+}$[d]	0.93	−1.23, −1.54

[a]All the potentials are referenced against Ag/AgCl electrode with $E_{1/2}$ = 0.36 V for Fc/Fc$^+$ couple. [b]Quasi-reversible electron transfer process with a Pt working electrode. [c]$E_{1/2}$ values obtained from square wave voltammetric (SWV) using glassy carbon electrode. [d]Data from ref 2. [e]Data from ref 45.

dx.doi.org/10.1021/ic401582m | Inorg. Chem. 2013, 52, 13941−13955

may be mentioned that the free tpy-HImzPy gets oxidized at 1.1 V.

Interaction of the Complexes with Anions in Solution. The sensing abilities of the metalloreceptors toward various anions such as F^-, Cl^-, Br^-, I^-, AcO^-, NO_3^-, ClO_4^-, and CN^- were studied in dimethysulfoxide solutions for **1**, **3**, and **4** and in acetonitrile solutions (2×10^{-5} M) for **2** . The interaction of **1**–**4** with HSO_4^- and $H_2PO_4^-$ could not be studied because of formation of a precipitate. Preliminary investigation revealed that a remarkable color change occur in all cases after addition of 10 equivalents F^-, AcO^-, and CN^- ions to their solutions. Figure 7 shows the prominent change in color of the

Figure 7. Color changes that occur when the solutions of **1**, **2**, and **4** are treated with various anions as their tetrabutylammonium (TBA) salts.

metalloreceptors in presence of F^- and CN^- and to a lesser extent with AcO^- ions. Conversely, the addition of equal quantity of the other anions such as Cl^-, Br^-, I^-, NO_3^-, and ClO_4^- failed to cause any significant color change. Thus, the metalloreceptors (**1**–**4**) are good colorimetric sensors for F^- and CN^- and comparably less for AcO^- ions.

Changes in the absorption spectral profiles of the complexes (**1**–**4**) upon addition of various anions were investigated by UV–vis spectrophotometeric measurements. Figure 8 and Figures S16–S17 (Supporting Information) show that on addition of 10 equiv. of Cl^-, Br^-, I^-, NO_3^-, and ClO_4^- to the solution of receptors (2×10^{-5} M), the MLCT band at 504 nm for **1** and 508 nm for **3** and **4** did not lead to any detectable change. But with similar addition of AcO^- ion, the said MLCT band shifted to 508, 516, and 517 nm for **1**, **3**, and **4**, respectively. In case of F^- and CN^-, upon addition of the same quantity of ions, the MLCT band further shifted to longer wavelength viz. 530 nm for **1**, 542 nm for **3**, and 541 nm for **4**. This is clearly demonstrated that the interaction between F^-, AcO^-, and CN^- ions and the receptors are significantly strong. The mode of interaction of receptor **2** with the anions is different compared to **1**, **3** and **4** as **2** possess different types of imidazole NH protons with varying acidities. Figure 8a shows that the MLCT band at 493 nm for **2** shifted to longer wavelength ranging between 522 and 537 nm upon addition of F^-, AcO^-, and CN^- ions. No such changes occur when other anions were added to the solution of **2**. The shifts of the MLCT bands of **1**–**4** to lower energy region are probably due to interactions (hydrogen bonding or proton transfer) between the imidazole NH proton(s) in the secondary coordination sphere of the coordinated tpy-HImzPy/H_2pbbzim moiety and the anions. When the extent of such interaction is very strong, proton transfer from the coordinated imidazole moiety to the

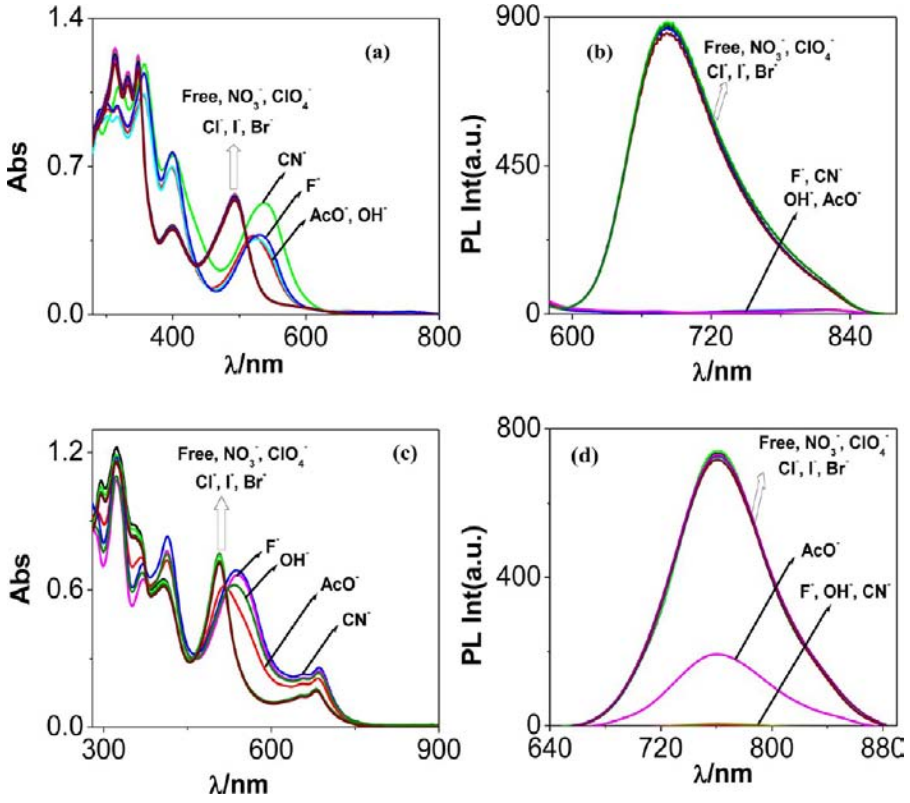

Figure 8. Changes in (a, c) UV–vis and (b, d) luminescence spectra of (a, b) **2** in acetonitrile and (c, d) **4** in dimethylsulfoxide upon the addition of different anions as TBA salts.

dx.doi.org/10.1021/ic401582m | *Inorg. Chem.* 2013, 52, 13941–13955

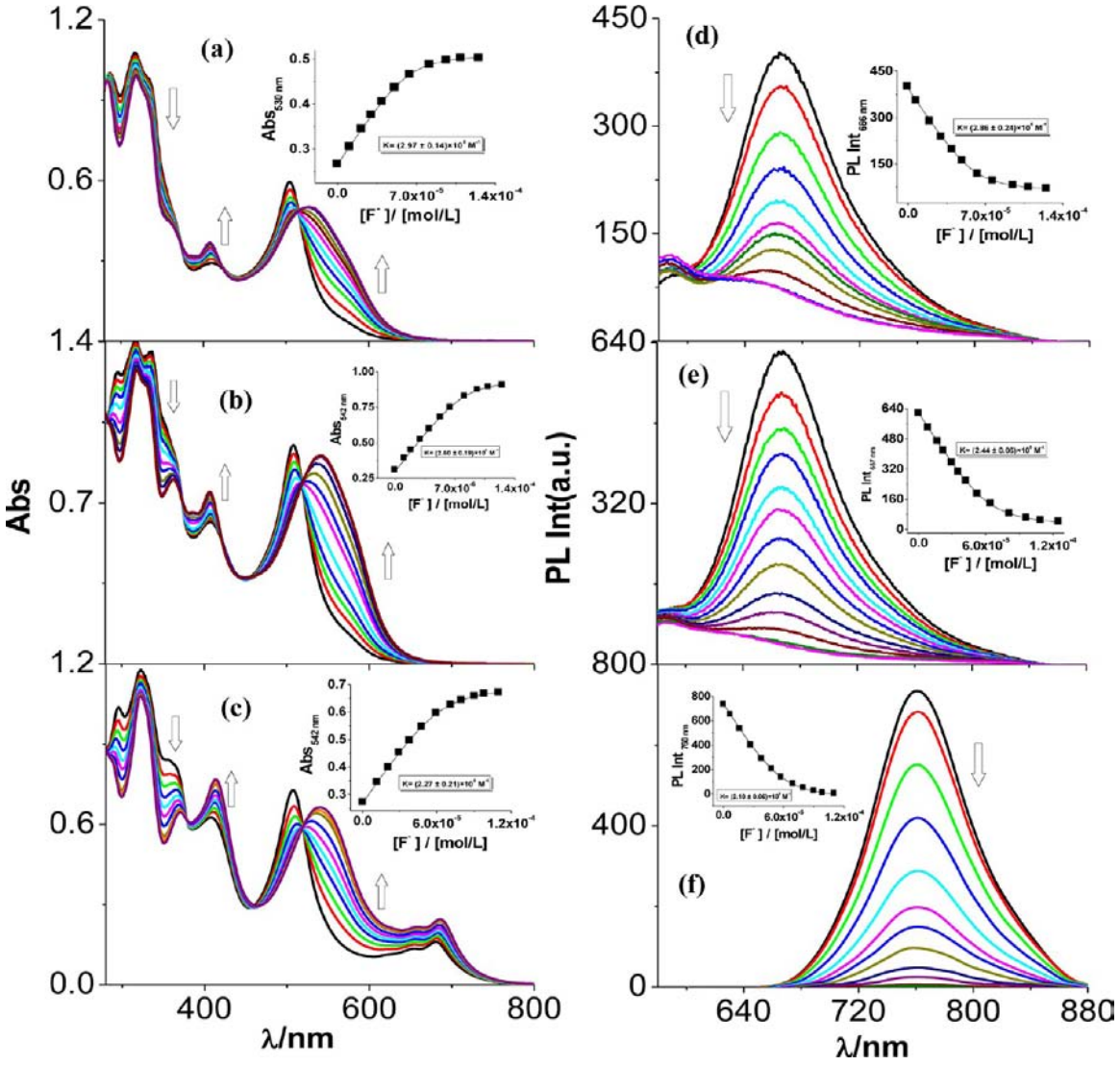

Figure 9. Changes in (a–c) absorption and (d–f) photoluminescence spectra of (a, d) **1**, (b, e) **3**, and (c, f) **4** in dimethylsulfoxide solution upon the addition of F^- ion. The inset shows the fit of the experimental absorbance and luminescence data to a 1:1 binding profile.

anions is more probable giving rise to the accumulation of negative charge on the ligand moiety and eventually on the metal center by delocalization of the negative charge through the aromatic frame. The increased electron density on the metal center is probably responsible for shifting the MLCT band to lower energies.[14,47]

Systematic UV–vis anion sensing titration experiments of **1**–**4** were performed by quantitative addition of various anions. Figure 9a–c shows the absorption spectral changes of **1**, **3**, and **4** with gradual addition of F^- ion. Upon incremental addition of F^- ion to the DMSO solution of **1**, the MLCT band at 504 nm was red-shifted to 530 nm with the emergence of three isosbestic points at 520, 421, and 372 nm (Figure 9a). Similar observations occur for **3** and **4** (Figure 9b, c). The successive absorption curves pass through three isosbestic points in both cases (520, 421, and 372 nm for **3** and 520, 462, and 378 nm for **4**) upon incremental addition of F^- ion and ultimately the MLCT band gets red-shifted from 508 to 542 nm for **3** and to 541 nm for **4**. Figures S18 and S19 (Supporting Information) represent the absorption spectral changes during the addition of CN^- and AcO^- ions to the solution of **1**, **3**, and **4**. It is evident that the MLCT band position shifted to a lesser extent for AcO^- compared with F^- and CN^- ions in all three cases. But the less basic anions do not lead to any spectral change because they are unable to deprotonate the NH proton(s) of the receptors.

Absorption spectral change for **2** is very interesting because of presence of different types of imidazole NH protons from two different ligand moieties. Figure 10 and Figures S20 and S21 (Supporting Information) represent the absorption spectral change upon incremental addition of CN^-, F^- and AcO^- respectively. From the UV–vis titration profiles, it is clear that two successive deprotonation step occur with incremental addition of the said ions. The first change takes place up to the addition of 1 equivalent CN^-, F^-, and AcO^-, indicating the formation of a 1:1 receptor–anion species. The second change, on the other hand, occurs with the addition of excess of CN^-, F^-, and AcO^- ions (Figure 10 and Figures S20–S21, Supporting Information). From the experimental data, it is clearly observed that relatively small amount of anions are required for **2** compared to **1**, **3**, and **4**. It may be noted from the absorption titration profiles that the successive deprotonation process for **2** occur from the NH protons of H_2pbbzim moiety, while tpy-HImzPy-based NH proton(s) get deproto-

dx.doi.org/10.1021/ic401582m | *Inorg. Chem.* 2013, 52, 13941–13955

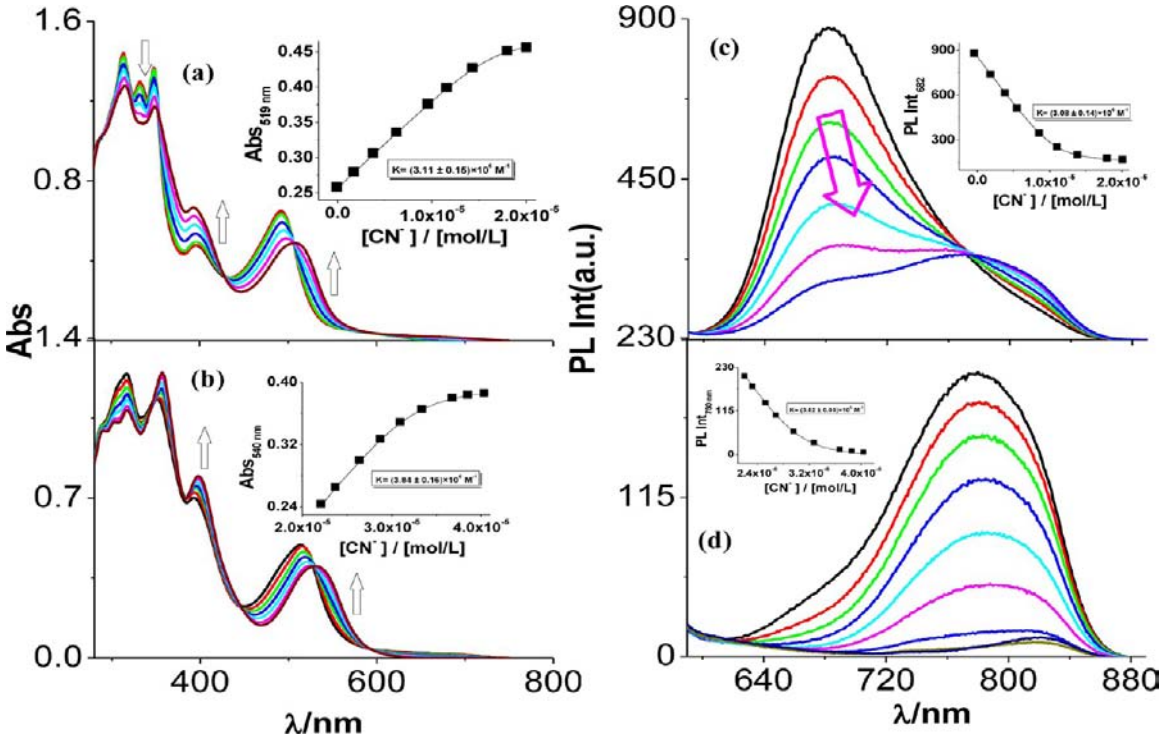

Figure 10. Changes in (a, b) absorption and (c, d) photoluminescence spectra of **2** in acetonitrile solution upon the addition of CN^- ion. The inset shows the fit of the experimental absorbance and luminescence data to a 1:1 binding profile.

Table 4. Equilibrium/Binding Constants[a,b] (K/M^{-1}) for 1, 3, and 4 in Dimethylsulfoxide and 2 in Acetonitrile towards Various Anions at 298 K

	1	2		3	4
anion	K	K_1	K_2	K	K
		From Absorption Spectra			
F^-	2.97×10^5	2.84×10^6	3.80×10^6	2.50×10^5	2.27×10^5
AcO^-	2.68×10^5	2.12×10^6	2.61×10^6	2.17×10^5	1.76×10^5
CN^-	3.69×10^5	3.11×10^6	3.84×10^6	3.54×10^5	2.85×10^5
		From Emission Spectra			
F^-	2.86×10^5	2.64×10^6	3.62×10^6	2.44×10^5	2.10×10^5
AcO^-	2.59×10^5	1.91×10^6	2.53×10^6	2.13×10^5	1.61×10^5
CN^-	3.57×10^5	3.08×10^6	3.52×10^6	3.48×10^5	2.75×10^5

[a] t-Butyl salts of the respective anions were used for the studies. [b] Estimated errors were <15%.

nated for **1**, **3**, and **4**. The equilibrium constants (K) of metalloreceptors toward different anions were determined from the absorption titrations data by using eq 1 and the values are compiled in Table 4.

Previous studies have established that when the basicity of the anion is high, deprotonation of the NH proton of the sensors became more favorable rather than strong hydrogen bonding interaction.[14,48,49] Thus, it is expected that in the presence of F^-, CN^-, and AcO^-, the imidazole NH proton(s) of the metalloreceptors will be deprotonated. Such possibility is confirmed by UV−vis absorption titrations of **1**-**4** with TBAOH (Figures S22 and S23, Supporting Information). The spectral changes are similar to that of F^- and CN^- for **1**, **3**, and **4** and F^-, AcO^-, and CN^- for **2**. These results indicate that the deprotonation process take place rather than hydrogen bonding interactions in all cases in presence of excess anions.

Anion sensing studies of **1**−**4** were also thoroughly investigated by emission spectroscopic measurements. In the absence of any anions, the characteristic emission maxima were observed at 665 nm for **1**, 668 nm for **3**, and 761 nm for **4** in DMSO. Upon addition of 10 equivalents Cl^-, Br^-, I^-, NO_3^-, and ClO_4^- ions, the emission maxima and intensities did not lead to any significant change (Figure 8d and Figures S16b−S17b, Supporting Information). By contrast, similar addition of F^- and CN^- ions to the solution of **1**, **3**, and **4** leads to almost complete quenching of the luminescence intensities. AcO^- ion, on the other hand, was unable to quench completely (Figure 8d and Figures S16b−S17b, Supporting Information). In the case of **2**, upon addition of F^-, AcO^-, and CN^- to its acetonitrile solution, again almost complete quenching along with considerable red-shift of the luminescence maximum from 682 to 820 nm occur (Figure 8b). Figures 9 and 10 and Figures S18−S21 (Supporting Information) show the luminescence spectral changes of **1**−**4** on gradual addition of F^-, AcO^-, and CN^- ions to their respective solutions. The equilibrium constants (Ks) of the receptors were also evaluated from the fluorometric titration data (Table 4), which were found to be in good agreement with the absorbance data. Table 4 indicates

dx.doi.org/10.1021/ic401582m | Inorg. Chem. 2013, 52, 13941−13955

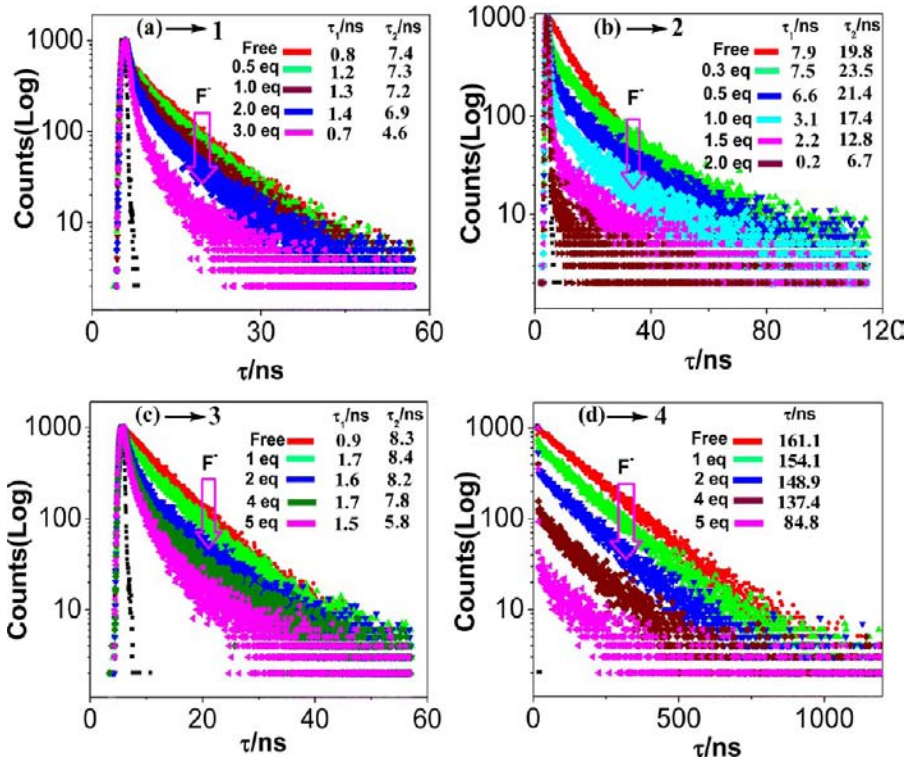

Figure 11. Changes in the time-resolved luminescence decays for (a) **1**, (c) **3**, and (d) **4** in dimethylsulfoxide and for (b) **2** in acetonitrile at room temperature upon the incremental addition of F^- ion.

that *K* values of **1**−**4** with F^-, CN^-, and AcO^- are grossly over 5 orders of magnitude. Moreover, considering the *K* values of a particular receptor, the general order of sensitivity is grossly the following: CN^- > F^- > AcO^-. The effects of incremental addition of TBAOH on the luminescence spectra of the metalloreceptors were also observed (Figures S22 and S23, Supporting Information). Close similarities of the spectral patterns between OH^- and F^-, CN^-, and AcO^- ions support the deprotonation mechanism.

The sensing behaviors of the luminescent transition metal complexes are very interesting because of their considerably long lifetimes compared to their purely organic counterparts.[50,51] Luminescence response of metalloreceptors on binding to various anions were also confirmed by time-resolved emission studies. Figure 11 shows the changes of luminescence lifetimes upon gradual addition of F^- ion to the solution of **1**−**4**. Initially, the luminescence decays of the three ruthenium(II) receptors (**1**−**3**) are found to be biexponential in nature, whereas **4** exhibits single exponential decay (Figure 11). In the case of **1** and **3**, the lifetime decreases gradually with increasing concentration of F^- ion (lifetimes are given in the inset of Figure 11). On the other hand, for **2**, during the initial two additions of the ions, the lifetimes of the first component decrease, whereas those of the second components increase to some extent. On further addition of F^- ion, the lifetimes of both first and second component decrease gradually. Figure 11d shows that in the presence of F^- ion, the luminescence decays of **4** are double exponential, with a short component having a decay constant comparable to the lamp profile and a long component with a lifetime gradually decreasing with incremental addition of F^- ion. These data suggest that on progressive addition of F^-, deprotonation process occurs and the lifetimes of the deprotonated species became shorter in general than that of the free receptors and the net result is the observed lifetime quenching as shown in Figure 11. It should be mentioned that the quenching effect of lifetimes makes the receptors good lifetime-based sensors for selective anions.

All the metalloreceptos show good selectivity for F^-, AcO^-, and CN^- ions compared to other anions which is evident from significant visual color change as well as remarkable absorption and emission spectral changes. Another important aspect of anion sensing is the detection limit of the sensors. Absorption and luminescence titrations data were utilized for evaluation of the detection limit of **1**−**4** (Figures S24−S29, Supporting Information).[52,53] The lower limit of detection for the above-mentioned ions lie in the range of 1×10^{-8} M to 1×10^{-9} M (Table S5, Supporting Information).

To further confirm the interaction between the metalloreceptors and anions, ^1H NMR titration experiments were also carried out in DMSO-d_6 solution. The spectral changes of **2** upon incremental addition of F^- ion up to 3 equiv. were presented in Figure 12. In the absence of F^- ion, a sharp singlet was observed at δ 15.07 ppm due to NH group. On addition of up to 0.8 equiv of F^- ion, the signal gets initially broadened and ultimately disappeared. During the addition of F^- ion between 0.8 and 2.0 equiv., a new peak evolved at 14.02 ppm, which can be assigned to NH group of coordinated tpy-HImzPy moiety. The signal at 14.02 ppm again disappeared on addition of 3 equiv. of F^- ion. It is worth noting in Figure 12 that the integrated proportion of the N−H signal initially at 15.07 ppm and thereafter at 14.02 ppm decreased progressively with the chemical shift remaining almost stable, indicating a typical proton transfer process.[31f,g,54] Importantly, the signals due to H20···H25 protons of H_2pbbzim and H3, H7, and H8 of tpy-HImzPy moieties exhibit progressive upfield-shift with increasing concentration of F^- ion (Figure 12). Figures S30−

dx.doi.org/10.1021/ic401582m | *Inorg. Chem.* 2013, 52, 13941−13955

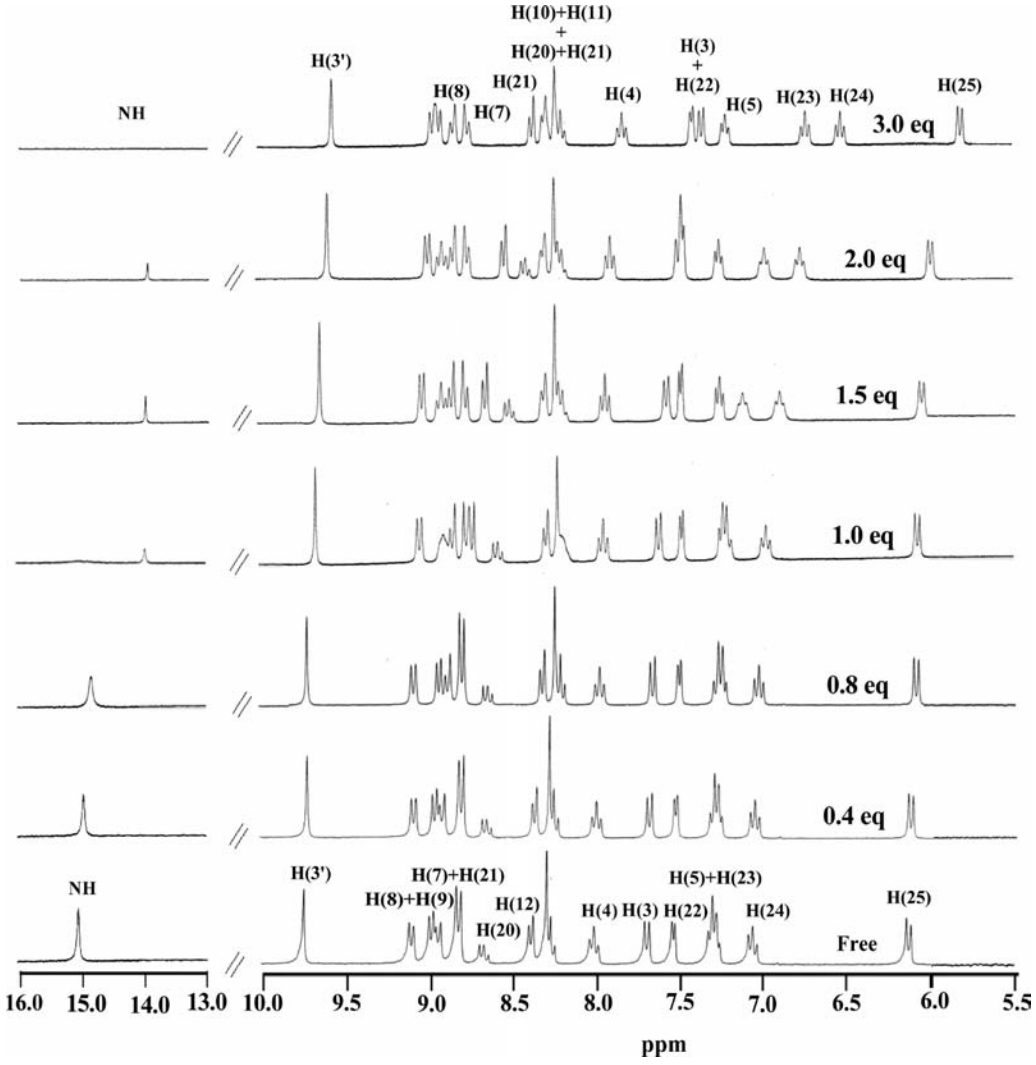

Figure 12. ^{1}H NMR titration of sensor **2** in DMSO-d_6 solution (5.0×10^{-3} M) upon addition of F^- ion (1.50×10^{-1} M, 0–3 equiv.).

S32 (Supporting Information) represent the ^{1}H NMR spectra of **1**, **3**, and **4** with addition of 5 equiv. of F^- ion. In all cases, the signal due to NH group lying between 13.98 and 15.07 ppm vanished with concomitant upfield shift of selective protons of tpy-HImzPy and H_2pbbzim moieties. The upfield shifts are due to the accumulation of the negative charge in the aromatic frame of the ligands arising out of the deprotonation of the NH groups.[14]

Cyclic and square wave voltammetry were used to study the electrochemical anion recognition properties of metalloreceptors in CH_3CN solution. Typically, Figure 13 shows the cyclic voltammograms of **2** on incremental addition of F^- ion. The oxidation potential of **2** at 1.05 V shifted to less positive direction with an emergence of a new oxidation peak at 0.50 V up to the addition of 3 equivalents of F^- ion. The current intensities of the new anodic peak around 0.50 V increase linearly with the equivalent of added F^- ion. Figures S33 and S34 (Supporting Information) represent the cyclic voltammograms of **1** and **3**, respectively, in the presence of excess F^- ion in CH_3CN solution. In all cases, the oxidation potentials shifted to lower potential region in presence of the anion. The increased electron density on the metal center arising out of the deprotonation of the NH groups in the presence of anions is probably responsible for lowering the oxidation potentials.[14,47]

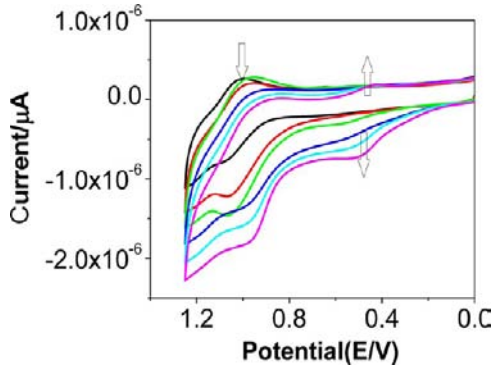

Figure 13. CVs of **2** obtained upon incremental addition of F^- ion (2.0×10^{-2} M) to its acetonitrile solution (2.5×10^{-4} M).

Finally, X-ray crystallographic study provided unambiguous proof for the deprotonation process of NH group(s) in the metalloreceptors by selective anions such as F^-. X-ray crystal structure determination of **2** in presence of excess TBAF revealed that the molecular structure of the resulting compound is [(pbbzim)Ru(tpy-HImzPy)] (**2a**), where two NH protons have been abstracted from H_2pbbzim moiety. ORTEP representation of **2a** was already shown in Figure 1b and the

dx.doi.org/10.1021/ic401582m | *Inorg. Chem.* 2013, 52, 13941–13955

pertinent crystallographic data along with selected bond distances and angles were summarized in Table 1 and Table S1 (Supporting Information).

CONCLUSION

In the present study, we have designed a new terpyridyl ligand rigidly link to pyrenyl-benzimidazole moiety (tpy-HImzPy) and utilized the ligand for the synthesis of a new family of homo- and heteroleptic bis-tridentate ruthenium(II) and osmium(II) complexes in combination with other tridentate ligands such as 4′-(2-naphthyl)-2,2′:6′,2″-terpyridine (tpy-NaPh) and 2,6-bis-(benzimidazole-2-yl)pyridine (H_2pbbzim). The absorption, steady-state, and time-resolved luminescence and electrochemical properties of all the complexes were thoroughly investigated. The photophysical properties of the metal complexes used in this study are much better than those of the parent $[M(tpy)_2]^{2+}$. In particular, all the three ruthenium(II) complexes exhibit moderately strong room temperature luminescence with excited-state lifetimes lying in the range of 3.8−69.3 ns. We believe that the energy of the ^{3}MC states of the complexes in the present study remain constant, while the energy of the emitting ^{3}MLCT state being lowered by rigidly connecting the pyrenyl-imidazole group to the terpyridine moiety and thereby enhancing the MLCT-MC energy gap. A point of interest is also that the physicochemical properties of the complexes are strongly perturbed by selective anions. Consequently, the anion sensing properties of the complexes have been thoroughly studied through different channels. It has been nicely demonstrated in this study that metals, even when coordinatively saturated, can play a valuable role in anion recognition, by enhancing the H-bond donor tendencies of a covalently linked imidazole N−H containing receptor. Such an enhancing effect can be modulated by varying the nature of the metal as well as the coordinated ligands. Spectrophotometric, steady state and time-resolved fluorimetric, ^{1}H NMR spectroscopic, cyclic voltammetric, and X-ray crystallographic studies provided evidence in favor of anion-induced deprotonation of the imidazole NH proton(s) of the complexes in the presence of selective anions.

ASSOCIATED CONTENT

Supporting Information

CIF files of the two crystal structures along with different figures related to ESI mass spectra, NMR, crystal structures, UV−vis, steady-state, and time-resolved luminescence spectral change as a function of different anions, CVs, and detection limit. This material is available free of charge via the Internet at http://pubs.acs.org.

AUTHOR INFORMATION

Corresponding Author

*E-mail: sbaitalik@hotmail.com.

Notes

The authors declare no competing financial interest.

ACKNOWLEDGMENTS

We gratefully acknowledge the financial support for this work from DST and CSIR, Government of India through project SR/S1/IC-33/2010 and 01(2084)/06/EMR-II, respectively. The X-ray diffractometer facility under the DST-FIST and TCSPC facility under the DST-PURSE programs of Department of Chemistry (JU) are also gratefully acknowledged. Dinesh Maity and Debiprasad Mondal would also like to thank CSIR for their fellowship.

REFERENCES

(1) (a) Balzani, V.; Credi, A.; Venturi, M. *Molecular Devices and Machines*; Wiley-VCH: Weinheim, Germany, 2003. (b) Sun, L.; Hammarström, L.; Akermark, B.; Styring, S. *Chem. Soc. Rev.* **2001**, *30*, 36. (c) Baitalik, S.; Wang, X.; Schmehl, R. H. *J. Am. Chem. Soc.* **2004**, *126*, 16304. (d) Liu, Y.; DeNicola, A.; Ziessel, R.; Schanze, K. S. *J. Phys. Chem. A.* **2003**, *107*, 3476. (e) Alstrum-Acevedo, J. H.; Brennaman, M. K.; Meyer, T. J. *Inorg. Chem.* **2005**, *44*, 6802. (f) Browne, W. R.; O'Boyle, N. M.; McGarvey, J. J.; Vos, J. G. *Chem. Soc. Rev.* **2005**, *34*, 641. (g) Balzani, V.; Clemente-Léon, M.; Credi, A.; Ferrer, B.; Venturi, M.; Flood, A. H.; Stoddart, J. F. *Proc. Natl. Acad. Sci. U.S.A.* **2006**, *103*, 1178. (h) Kuang, D.; Ito, S.; Wenger, B.; Klein, C.; Moser, J.-E.; Humphry-Baker, R.; Zakeeruddin, S. M.; Gratzel, M. *J. Am. Chem. Soc.* **2006**, *128*, 4146.

(2) (a) Juris, A.; Balzani, V.; Barigelletti, F.; Campagna, S.; Belser, P.; von Zelewsky, A. *Coord. Chem. Rev.* **1988**, *84*, 85. (b) Balzani, V.; Juris, A.; Venturi, M.; Campagna, S.; Serroni, S. *Chem. Rev.* **1996**, *96*, 759. (c) Sauvage, J.-P.; Collin, J. P.; Chambron, J. C.; Guillerez, S.; Coudret, C.; Balzani, V.; Barigelletti, F.; De Cola, L.; Flamigni, L. *Chem. Rev.* **1994**, *94*, 993.

(3) (a) Meyer, T. J. *Pure Appl. Chem.* **1986**, *58*, 1193. (b) Meyer, T. J. *Acc. Chem. Res.* **1989**, *22*, 163.

(4) Winkler, J. R.; Netzel, T.; Creutz, C.; Sutin, N. *J. Am. Chem. Soc.* **1987**, *109*, 2381.

(5) (a) Knof, U.; von Zelewsky, A. *Angew. Chem., Int. Ed.* **1999**, *38*, 302. (b) Bodige, S.; Kim, M. −J.; MacDonnell, F. M. *Coord. Chem. Rev.* **1999**, *185−186*, 535. (c) Keene, F. R. *Chem. Soc. Rev.* **1998**, *27*, 185.

(6) (a) Constable, E. C. *Chem. Soc. Rev.* **2007**, *36*, 246. (b) Hofmeier, H.; Schubert, U. S. *Chem. Soc. Rev.* **2004**, *33*, 373. (c) Medlycott, E. A.; Hanan, G. S. *Coord. Chem. Rev.* **2006**, *250*, 1763. (d) Medlycott, E. A.; Hanan, G. S. *Chem. Soc. Rev.* **2005**, *34*, 133. (e) Wang, X.-Y.; Del Guerzo, A.; Schmehl, R. H. J. *Photochem. Photobiol. C.* **2004**, *5*, 55.

(7) (a) Maestri, M.; Armaroli, N.; Balzani, V.; Constable, E. C.; Thompson, A. M. W. C. *Inorg. Chem.* **1995**, *34*, 2759. (b) Wang, J.; Fang, Y. Q.; Hanan, G. S.; Loiseau, F.; Campagna, S. *Inorg. Chem.* **2005**, *44*, 5.

(8) (a) Fang, Y. Q.; Taylor, N. J.; Hanan, G. S.; Loiseau, F.; Passalacqua, R.; Campagna, S.; Nierengarten, H.; Van Dorsselaer, A. *J. Am. Chem. Soc.* **2002**, *124*, 7912. (b) Passalacqua, R.; Loiseau, F.; Campagna, S.; Fang, Y. Q.; Hanan, G. S. *Angew. Chem., Int. Ed.* **2003**, *42*, 1608. (c) Polson, M. I. J.; Loiseau, F.; Campagna, S.; Hanan, G. S. *Chem. Commun.* **2006**, 1301. (d) Fang, Y. Q.; Taylor, N. J.; Laverdiere, F.; Hanan, G. S.; Loiseau, F.; Nastasi, F.; Campagna, S.; Nierengarten, H.; Leize-Wagner, E.; Van Dorsselaer, A. *Inorg. Chem.* **2007**, *46*, 2854.

(9) (a) Hissler, M.; El-ghayoury, A.; Harriman, A.; Ziessel, R. *Angew. Chem., Int. Ed.* **1998**, *37*, 1717. (b) Encinas, S.; Flamigni, L.; Barigelletti, F.; Constable, E. C.; Housecroft, C. E.; Schofield, E. R.; Figgemeier, E.; Fenske, D.; Neuburger, M.; Vos, J. G.; Zehnder, M. *Chem.—Eur. J.* **2002**, *8*, 137. (c) Benniston, A. C.; Harriman, A.; Li, P.; Sams, C. A. *J. Am. Chem. Soc.* **2005**, *127*, 2553. (d) Wang, X-y.; Del Guerzo, A.; Tunuguntla, H.; Schmehl, R. H. *Res. Chem. Intermed.* **2007**, *33*, 63.

(10) (a) Duati, M.; Fanni, S.; Vos, J. G. *Inorg. Chem. Commun.* **2000**, *3*, 68. (b) Duati, M.; Tasca, S.; Lynch, F. C.; Bohlen, H.; Vos, J. G.; Stagni, S.; Ward, M. D. *Inorg. Chem.* **2003**, *42*, 8377.

(11) (a) Constable, E. C.; Dunne, S. J.; Rees, D. G. F.; Schmitt, C. X. *Chem. Commun.* **1996**, 1169. (b) Indelli, M. T.; Bignozzi, C. A.; Scandola, F.; Collin, J.-P. *Inorg. Chem.* **1998**, *37*, 6084.

(12) (a) Beley, M.; Collin, J.-P.; Louis, R.; Metz, B.; Sauvage, J.-P. *J. Am. Chem. Soc.* **1991**, *113*, 8521. (b) Wilkinson, A. J.; Puschmann, H.; Howard, J. A. K.; Foster, C. E.; Williams, J. A. G. *Inorg. Chem.* **2006**, *45*, 8685. (c) Wadman, S. H.; Lutz, M.; Tooke, D. M.; Spek, A. L.; Hartl, F.; Havenith, R.W. A.; van Klink, G. P. M.; van Koten, G. *Inorg. Chem.* **2009**, *48*, 1887.

(13) (a) Abrahamsson, M.; Jäger, M.; Österman, T.; Eriksson, L.; Persson, P.; Becker, H. C.; Johansson, O.; Hammarström, L. *J. Am.*

Chem. Soc. **2006**, *128*, 12616. (b) Abrahamsson, M.; Jäger, M.; Kumar, R. J.; Österman, T.; Persson, P.; Becker, H. C.; Johansson, O.; Hammarström, L. *J. Am. Chem. Soc.* **2008**, *130*, 15533.
(14) (a) Bhaumik, C.; Das, S.; Saha, D.; Dutta, S.; Baitalik, S. *Inorg. Chem.* **2010**, *49*, 5049. (b) Bhaumik, C.; Saha, D.; Das, S.; Baitalik, S. *Inorg. Chem.* **2011**, *50*, 12586. (c) Bhaumik, C.; Das, S.; Maity, D.; Baitalik, S. *Dalton Trans.* **2012**, *41*, 2427. (d) Bhaumik, C.; Das, S.; Maity, D.; Baitalik, S. *Dalton Trans.* **2011**, *40*, 11795. (e) Bhaumik, C.; Das, S.; Maity, D.; Baitalik, S. *RSC Adv.* **2012**, *2*, 2581. (f) Bhaumik, C.; Maity, D.; Das, S.; Baitalik, S. *Polyhedron* **2013**, *52*, 890.
(15) (a) Wrighton, M. S.; Morse, D. L.; Pdungsap, L. *J. Am. Chem. Soc.* **1975**, *97*, 2073. (b) Giordano, P. J.; Fredericks, S. M.; Wrighton, M. S.; Morse, D. L. *J. Am. Chem. Soc.* **1978**, *100*, 2257. (c) Fredericks, S. M.; Luong, J. C.; Wrighton, M. S. *J. Am. Chem. Soc.* **1979**, *101*, 7415.
(16) Ford, W. E.; Rodgers, M. A. J. *J. Phys. Chem.* **1992**, *96*, 2917.
(17) (a) Wilson, G. J.; Sasse, W. H. F.; Mau, A. W. H. *Chem. Phys. Lett.* **1996**, *250*, 583. (b) Wilson, G. J.; Launikonis, A.; Sasse, W. H. F.; Mau, A. W. H. *J. Phys. Chem. A* **1997**, *101*, 4860. (c) Wilson, G. J.; Launikonis, A.; Sasse, W. H. F.; Mau, A. W. H. *J. Phys. Chem. A* **1998**, *102*, 5150.
(18) (a) Grusenmeyer, T. A.; Chen, J.; Jin, Y.; Nguyen, J.; Rack, J. J.; Schmehl, R. H. *J. Am. Chem. Soc.* **2012**, *134*, 7497. (b) Gu, J.; Chen, J.; Schmehl, R. H. *J. Am. Chem. Soc.* **2010**, *132*, 7338. (c) Simon, J. A.; Curry, S. L.; Schmehl, R. H.; Schatz, T. R.; Piotrowiak, P.; Jin, X.; Thummel, R. P. *J. Am. Chem. Soc.* **1997**, *119*, 11012. (d) Balazs, G. C.; del Guerzo, A.; Schmehl, R. H. *Photochem. Photobiol. Sci.* **2005**, *4*, 89. (e) Schmehl, R. *Spectrum* **2000**, *13*, 17. (f) Del Guerzo, A.; Leroy, S.; Fages, F.; Schmehl, R. H. *Inorg. Chem.* **2002**, *41*, 359.
(19) (a) Tyson, D. S.; Castellano, F. N. *J. Phys. Chem. A* **1999**, *103*, 10955. (b) Tyson, D. S.; Castellano, F. N. *Chem. Commun.* **2000**, 2355. (c) Tyson, D. S.; Henbest, K. B.; Bialecki, J.; Castellano, F. N. *J. Phys. Chem. A* **2001**, *105*, 8154. (d) Tyson, D. S.; Luman, C. R.; Zhou, X.; Castellano, F. N. *Inorg. Chem.* **2001**, *40*, 4063.
(20) (a) Harriman, A.; Hissler, M.; Khatyr, A.; Ziessel, R. *Chem. Commun.* **1999**, 735. (b) Hissler, M.; Harriman, A.; Khatyr, A.; Ziessel, R. *Chem.—Eur. J.* **1999**, *5*, 3366. (c) Benniston, A. C.; Harriman, A.; Lawrie, D. J.; Mayeux, A. *Phys. Chem. Chem. Phys.* **2004**, *6*, 51.
(21) Sohna Sohna, J.; Carrier, V.; Fages, F.; Amouyal, E. *Inorg. Chem.* **2001**, *40*, 6061.
(22) Ji, S.; Wu, W.; Wu, W.; Guo, H.; Zhao, J. *Angew. Chem., Int. Ed.* **2011**, *50*, 1626.
(23) (a) Morales, A. F.; Accorsi, G.; Armaroli, N.; Barigelletti, F.; Pope, S. J. A.; Ward, M. D. *Inorg. Chem.* **2002**, *41*, 6711. (b) Maubert, B.; McClenaghan, N. D.; Indelli, M. T.; Campagna, S. *J. Phys. Chem. A* **2003**, *107*, 447.
(24) Michalec, J. F.; Bejune, S. A.; McMillin, D. R. *Inorg. Chem.* **2000**, *39*, 2708.
(25) *Topics in Fluorescence Spectroscopy, Vol. 4: Probe Design and Chemical Sensing*; Lakowicz, J. R., Ed.; Plenum Press: New York, 1994.
(26) Balzani, V.; Scandola, F. *Supramolecular Photochemistry*; Horwood: Chichester, England, 1991.
(27) Lehn, J.-M. *Supramolecular Chemistry: Concepts and Perspectives* VCH: Weinheim, Germany, 1995.
(28) Maity, D.; Das, S.; Mardanya, S.; Baitalik, S. *Inorg. Chem.* **2013**, *52*, 6820.
(29) Beer, P. D.; Bayly, S. R. *Acc. Chem. Res.* **1998**, *31*, 71.
(30) Martínez-Máñez, R.; Sancenón, F. *Chem. Rev.* **2003**, *103*, 4419.
(31) (a) Beer, P. D.; Szemes, F.; Balzani, V.; Salà, C. M.; Drew, M. G. B.; Dent, S. W.; Maestri, M. *J. Am. Chem. Soc.* **1997**, *119*, 11864. (b) Beer, P. D.; Szemes, F. *J. Chem. Soc., Chem. Commun.* **1995**, 2245. (c) Szemes, F.; Hesek, D.; Chen, Z.; Dent, S. W.; Drew, M. G. B.; Goulden, A. J.; Graydon, A. R.; Grieve, A.; Mortimer, R. J.; Wear, T. J.; Weightman, J. S.; Beer, P. D. *Inorg. Chem.* **1996**, *35*, 5868. (d) Anzebacher, P.; Tyson, D. S.; Jurslkova, K.; Castellano, F. N. *J. Am. Chem. Soc.* **2002**, *124*, 6232. (e) Mizuno, T.; Wei, W.-H.; Eller, L. R.; Sessler, J. L. *J. Am. Chem. Soc.* **2002**, *124*, 1134. (f) Cui, Y.; Mo, H.-J.; Chen, J.-C.; Niu, Y.-L.; Zhong, Y.-R.; Zheng, K.-C.; Ye, B.-H. *Inorg. Chem.* **2007**, *46*, 6427. (g) Cui, Y.; Niu, Y.-L.; Cao, M. L.; Wang, K.; Mo, H.-J.; Zhong, Y.-R.; Ye, B.-H. *Inorg. Chem.* **2008**, *47*, 5616. (h) Lin, Z.-H.; Zhao, Y.-G.; Duan, C.-Y.; Zhang, B.-G.; Bai, Z.-P. *Dalton Trans.* **2006**, 3678. (i) Ion, L.; Morales, D.; Perez, J.; Riera, L.; Riera, V.; Kowenicki, R. A.; McPartlin, M. *Chem. Commun.* **2006**, 91. (j) Zapata, F.; Caballero, A.; Espinosa, A.; Tárraga, A.; Molina, P. *J. Org. Chem.* **2008**, *73*, 4034. (k) Derossi, S.; Adams, H.; Ward, M. D. *Dalton Trans.* **2007**, 33. (l) Lin, T.-P.; Chen, C.-Y.; Wen, Y.-S.; Sun, S.-S. *Inorg. Chem.* **2007**, *46*, 9201. (m) Jose, D. A.; Kar, P.; Koley, D.; Ganguly, B.; Thiel, W.; Ghosh, H. N.; Das, A. *Inorg. Chem.* **2007**, *46*, 5576.
(32) (a) Yam, V. W. W. *Acc. Chem. Res.* **2002**, *35*, 555. (b) Wong, K. M. C.; Tang, W. S.; Lu, X. X.; Zhu, N.; Yam, V. W. W. *Inorg. Chem.* **2005**, *44*, 1492. (c) Yam, V. W. W.; Tang, R. P. L.; Wong, K. M. C.; Lu, X. X.; Cheung, K. K.; Zhu, N. *Chem.- Eur. J.* **2002**, *8*, 4066. (d) Yam, V. W. W.; Wong, K. M. C.; Zhu, N. *Angew. Chem., Int. Ed.* **2003**, *42*, 1400.
(33) (a) Padilla-Tosta, M. E.; Lloris, J. M.; Martínez-Máñez, R.; Pardo, T.; Soto, J.; Benito, A.; Marcos, M. D. *Inorg. Chem. Commun.* **2000**, *3*, 45. (b) Padilla-Tosta, M. E.; Lloris, J. M.; Martínez-Máñez, R.; Pardo, T.; Sancenón, F.; Soto, J.; Marcos, M. D. *Eur. J. Inorg. Chem.* **2001**, 1221. (c) Calero, P.; Hecht, M.; Martinez-Manez, R.; Sancenon, F.; Soto, J.; Vivancos, J. L.; Rurack, K. *Chem. Commun.* **2011**, *47*, 10599.
(34) Baggi, G.; Boiocchi, M.; Ciarrocchi, C.; Fabbrizzi, L. *Inorg. Chem.* **2013**, *52*, 5273.
(35) Hu, J.; Zhang, D.; Harris, F. W. *J. Org. Chem.* **2005**, *70*, 707.
(36) Krohnke, F. *Synthesis* **1976**, *1*, 1−24.
(37) Schneider, H.-J.; Yatsimirsky, A. *Principles and Methods in Supramolecular Chemistry*; John Wiley & Sons: Chichester, U.K., 2000; p 142.
(38) *SAINT (version 6.02), SADABS (version 2.03)*; Bruker AXS Inc.: Madison, WI, 2002.
(39) Sheldrick, G. M. *SHELXL-97, Program for the Refinement of crystal Structures*; University of Göttingen: Göttingen, Germany, 1997.
(40) *SHELXTL, (version 6.10)*; Bruker AXS Inc.: Madison, WI, 2002.
(41) PLATON: Spek, A. L. *J. Appl. Crystallogr.* **2003**, *36*, 7−13.
(42) ORTEP-32 for Windows: Farrugia, L. J. *J. Appl. Crystallogr.* **1997**, *30*, 565.
(43) WinGX−A windows program for crystal structures analysis: Farrugia, L. J. *J. Appl. Crystallogr.* **1999**, *32*, 837.
(44) (a) Coe, B. J.; Thompson, D. W.; Culbertson, C. T.; Schoonover, J. R.; Meyer, T. *J. Inorg. Chem.* **1995**, *34*, 3385. (b) Kober, E. M.; Meyer, T. *J. Inorg. Chem.* **1982**, *21*, 3967.
(45) Xiaoming, X.; Haga, M.; Inoue, T. M.; Ru, Y.; Addison, A. W.; Kano, K. *J. Chem. Soc., Dalton Trans.* **1993**, 2477.
(46) Wang, J.; Hanan, G. S.; Loiseau, F.; Campagna, S. *Chem. Commun.* **2004**, 2068.
(47) (a) Balzani, V.; Sabbatini, N.; Scandola, F. *Chem. Rev.* **1986**, *86*, 319. (b) Rampi, M. A.; Indelli, M. T.; Scandola, F.; Pina, F.; Parola, A. J. *Inorg. Chem.* **1996**, *35*, 3355.
(48) (a) Kang, S. O.; Powell, D.; Day, V. W.; Bowman-James, K. *Angew. Chem., Int. Ed.* **2006**, *45*, 7882. (b) Gunnlaugasson, T.; Kruger, P. E.; Jensen, P.; Tierney, J.; Ali, H. D. P.; Hussey, G. M. *J. Org. Chem.* **2005**, *70*, 10875. (c) Gomez, D. E.; Fabbrizzi, L.; Licchelli, M. *J. Org. Chem.* **2005**, *70*, 5717. (d) Boiocchi, M.; Boca, L. D.; Gomez, D. E.; Fabbrizzi, L.; Licchelli, M.; Monzani, E. *Chem.—Eur. J.* **2005**, *11*, 3097.
(49) (a) Nishiyabu, R.; Anzenbacher, P., Jr. *J. Am. Chem. Soc.* **2005**, *127*, 8270. (b) Aldakov, D.; Palacios, M. A.; Anzenbacher, P. *Chem. Mater.* **2005**, *17*, 5238.
(50) Demas, J. N.; DeGraff, B. A. *Anal. Chem.* **1991**, *63*, 829A.
(51) Lakowicz, J. R. *Principles of Fluorescence Spectroscopy*, 2nd ed.; KluwerAcademic/Plenum Publishers: New York, 1999.
(52) Shortreed, M.; Kopelman, R.; Kuhn, M.; Hoyland, B. *Anal. Chem.* **1996**, *68*, 1414.
(53) Ding, Y.; Xie, Y.; Li, X.; Hill, J. P.; Zhang, W.; Zhu, W. *Chem. Commun.* **2011**, *47*, 5431.
(54) (a) Lin, Z.-H.; Ou, S.-J.; Duan, C.-Y.; Zhang, B.-G.; Bai, Z.-P. *Chem. Commun.* **2006**, 624. (b) Evans, L. S.; Gale, P. A.; Light, M. E.; Quesada, R. *Chem. Commun.* **2006**, 965.